
Research article

Enhanced fault detection models with real-life applications

Showkat Ahmad Lone¹, Zahid Rasheed^{2,3}, Sadia Anwar⁴, Majid Khan^{5,*}, Syed Masroor Anwar⁶ and Sana Shahab⁷

¹ Department of Basic Science, College of Science and Theoretical Studies, Saudi Electronic University, 11673, KSA

² School of Mathematics and Statistics, Xi'an Jiaotong University, 710049, China

³ Department of Mathematics, Women University of Azad Jammu and Kashmir, Bagh, AJ&K, 12500, Pakistan

⁴ Department of Mathematics, College of Arts & Sciences (Wadi Addawasir), Prince Sattam Bin Abdulaziz University, Alkharj, Saudi Arabia

⁵ Government Akhtar Nawaz Khan (Shaheed) Degree College, KTS, Haripur, KPK, 22800, Pakistan

⁶ Department of Statistics, University of Azad Jammu and Kashmir, Muzaffarabad, 13100, Pakistan

⁷ Department of Business Administration, College of Business Administration, Princes Nourah Bint Abdulrahman University P.O Box 84428, Riyadh, 11671, Saudi Arabia

***Correspondence:** Email: 285004majidkhan@gmail.com.

Abstract: Nonconforming events are rare in high-quality processes, and the time between events (TBE) may follow a skewed distribution, such as the gamma distribution. This study proposes one- and two-sided triple homogeneously weighted moving average charts for monitoring TBE data modeled by the gamma distribution. These charts are labeled as the THWMA TBE charts. Monte Carlo simulations are performed to approximate the run length distribution of the one- and two-sided THWMA TBE charts. The THWMA TBE charts are compared to competing charts like the DHWMA TBE, HWMA TBE, THWMA TBE, DEWMA TBE, and EWMA TBE charts at a single shift and over a range of shifts. For the single shift comparison, the average run length (ARL) and standard deviation run length (SDRL) measures are used, whereas the extra quadratic loss (EQL), relative average run length (RARL) and performance comparison index (PCI) measures are employed for a range of shifts comparison. The comparison reveals that the THWMA TBE charts outperform the competing charts at a single shift as well as at a certain range of shifts. Finally, two real-life data applications are presented to evaluate the applicability of the THWMA TBE charts in practical situations, one with boring machine failure data and the other with hospital stay time for traumatic brain injury patients.

Keywords: average run length; extra quadratic loss; fault detection; high-quality process; process monitoring

Mathematics Subject Classification: 62P30

1. Introduction

Statistical process monitoring (SPM) tools are a set of instruments utilized for monitoring the quality of products in manufacturing and production processes. In these instruments, the charts are more vital tools that detect changes in process parameter(s). Shewhart [1] introduced the basic charts, which are referred to as the Shewhart charts. The Shewhart charts for attribute data, such as c , p and u charts, are used to monitor the nonconforming events. Despite being user-friendly, the Shewhart attribute charts tend to be insensitive in monitoring nonconforming events, particularly in high-quality processes. High-quality processes consistently produce products or services that meet or exceed customer expectations while minimizing waste and maximizing efficiency and have very low numbers of nonconforming events. In such processes, apart from monitoring nonconforming events, an alternate strategy is to utilize a chart to monitor the inter-arrival time of nonconforming events, which may follow a skewed distribution such as the gamma distribution. Time between events (TBE) charts are typically preferred over the Shewhart charts for high-quality processes where nonconforming events rarely occur [2,3].

In literature, many studies have been conducted that investigate TBE charts. For example, Lucas [4] proposed the cumulative sum (CUSUM) chart for exponentially distributed TBE data. Later, Vardeman and Ray [5] used integral equations to compute the average run length (ARL) for the exponential CUSUM chart. Gan [6] introduced the exponentially weighted moving average (EWMA) chart based on the exponential distribution. Chan et al. [7] designed the Shewhart-type chart, i.e., the cumulative quantity control (CQC) chart, or t -chart, to monitor the exponentially distributed TBE. Xie et al. [8] designed the Shewhart-type chart, i.e., the t_r -chart for monitoring the r th ($r \geq 1$) failures in the gamma distribution. Pehlivan and Testik [9] investigated the robustness of the exponential EWMA chart, where the TBE mean is assumed to be known; but, TBE observations are modeled by Weibull or lognormal distribution. Chakraborty et al. [10] proposed the gamma distribution-based lower-sided generally weighted moving average (GWMA) chart, called the GWMA TBE chart, that monitors downward changes in TBE data. Alevizakos et al. [2] improved the performance of the GWMA TBE chart and proposed the lower-sided double GWMA chart, referred to as the DGWMA TBE chart. Alevizakos and Koukouvinos [11] designed the double EWMA chart, referred to as the DEWMA TBE chart, that outperforms the EWMA TBE chart in monitoring downward changes in the process. Alevizakos et al. [12] developed one- and two-sided triple EWMA chart to monitor the TBE data, referred to as the TEWMA TBE chart.

Roberts [13] introduced the traditional EWMA chart, which monitors the mean level of the process. In general, the EWMA chart is more sensitive than the Shewhart-type chart in identifying small changes in the process as it uses both current and previous process observations. However, the EWMA chart allocates relatively more weight to recent process observations than previous observations [14]. As a result, Abbas [15] proposed the homogeneously weighted moving average (HWMA) chart for monitoring process mean, which outperforms the EWMA chart. Abid et al. [16] extended the concept of the HWMA chart and proposed the double HWMA (DHWMA) chart. Riaz

et al. [17] introduced the triple HWMA (THWMA) chart for the mean level of the process that improves the detection ability of the HWMA and DHWMA charts. Other charts based on the HWMA statistic are proposed in the studies of Rasheed et al. [18], Rasheed et al. [19] and Rasheed et al. [20].

As stated previously, Chakraborty et al. [10], Alevizakos et al. [2] and Alevizakos and Koukouvinos [11] introduced the one-sided GWMA TBE, DGWMA TBE and DEWMA TBE charts, respectively, for monitoring TBE observations following the gamma distribution. Aslam et al. [3] proposed the HWMA chart to monitor the TBE, referred to as the HWMA TBE chart. These charts are lower-sided charts that effectively monitor only the process's downward shifts (i.e., process deterioration). In practice, however, both downward shifts and upward shifts (i.e., process improvement) in the process must be monitored because corrective actions must be taken in both cases, either to diagnose and remove the causes of the process deterioration or to detect and maintain the reasons of the process improvements. As a result, in high-quality processes, a two-sided chart that monitors both downward and upward shifts at the same time is required. In this regard, Alevizakos et al. [12], Alevizakos and Koukouvinos [21] and Alevizakos and Koukouvinos [22] suggested the gamma distribution-based two-sided TEWMA TBE, provisional mean TBE (PM TBE) and double PM TBE (DPM TBE) charts, which monitor both the process's downward and upward shifts. These charts may indicate that the process performance needs to be improved further. To enhance the performance of TBE charts, this study proposes the design structures of one-sided (upper and lower) and two-sided THWMA charts with time-varying control limits that efficiently monitor the gamma-distributed TBE observations. The proposed charts are referred to as THWMA TBE charts. The lower-sided THWMA TBE chart is designed to detect downward shifts in the process, while the upper-sided THWMA TBE chart is constructed to monitor upwards changes in the process. Similarly, the two-sided THWMA TBE chart is developed to detect both downwards and upwards shifts in the process. Extensive Monte Carlo simulations are used to compute the numerical finding associated with the THWMA TBE charts. In parallel to THWMA TBE charts, the one- and two-sided competing TBE charts, such as the DHWMA TBE, HWMA TBE, TEWMA TBE, DEWMA TBE and EWMA TBE charts, are also constructed for comparison purposes. The proposed charts are compared to competing charts. The comparison of the THWMA TBE charts to the competing TBE charts suggests that the competing TBE charts perform better than the competing TBE charts in detecting changes in the process. Lastly, two applications, i.e., boring machine failure data and traumatic brain injury patients' hospital stay time data applications are provided to assess the THWMA TBE charts practically.

The layout for the rest of the article is as follows: Section 2 describes the methodologies of the gamma-distributed THWMA TBE charts, along with several competing charts. Section 3 offers the design and implementation of the THWMA TBE charts. Performance and comparison analysis of the THWMA TBE charts are provided in Section 4. Section 5 presents the two real-life applications of the THWMA TBE chart. The last section addresses the overall summary, conclusions and recommendations of the study.

2. Gamma-distributed TBE charts

In this section, an introduction to gamma-distributed *TBE* observations is provided in Subsection 2.1. The construction of the one- and two-sided TBE, DEWMA TBE, TEWMA TBE,

HWMA TBE and DHWMA TBE charts is outlined in Subsections 2.2 to 2.6, respectively. Likewise, Subsection 2.7 explains the methodology and formulation of the proposed one- and two-sided THWMA TBE charts.

2.1. Gamma-distributed TBE observations

Let $T_1^*, T_2^*, \dots, T_k^*$ represent the interarrival times between two successive occurrences in a homogeneous Poisson process having a rate of $\theta^{-1} (\theta > 0)$. In this case, each T_i^* is known as an independently and identically distributed (iid) exponential random variable with scale parameter θ , i.e., $T_i^* \stackrel{iid}{\sim} \text{Exponential}(\theta)$ for $i = 1, 2, \dots, k$. If T denotes the sum of interarrival times until the first k failures occur, i.e., $T = \sum_{i=1}^k T_i^*$, then T follows the gamma distribution, i.e., $T \sim \text{Gamma}(k, \theta)$. The probability density function (pdf) of T , is given as follows:

$$f_T(r; k, \theta) = \frac{r^{k-1}}{\Gamma(k)\theta^k} \exp\left(-\frac{r}{\theta}\right); r, k, \theta > 0, \quad (1)$$

where $\Gamma(\cdot)$ is called the gamma function, k (assumed known) is a shape parameter and θ is a scale parameter of the gamma distribution. The mean and variance of the gamma distribution are $k\theta$ and $k\theta^2$, respectively. The gamma distribution defined by Eq (1) is also referred to as the Erlang distribution. It is important to note that if $k = 1$, then gamma (k, θ) reduces to exponential(θ). In this case, the interest only lies in monitoring the time until one failure occurs.

Let $T_t \stackrel{iid}{\sim} \text{Gamma}(k, \theta)$ at time $t = 1, 2, \dots$ having mean and variance $k\theta$ and $k\theta^2$, respectively. The process is deemed to be in control (IC) when $\theta = \theta_0$; otherwise, if $\theta = \theta_1$ then the process is said to be out-of-control (OOC). In the OOC process, if $\theta_1 < \theta_0$ then the process is considered to have deteriorated; however, if $\theta_1 > \theta_0$ then the process may have improved. In both scenarios, corrective action should be taken to diagnose (if any $\theta_1 < \theta_0$) or preserve (if any $\theta_1 > \theta_0$) the reasons for change.

2.2. EWMA TBE chart

The EWMA TBE chart is defined by the charting statistic, X_t and can be defined as follows:

$$X_t = \varphi T_t + (1 - \varphi)X_{t-1}, \quad t = 1, 2, \dots, \quad (2)$$

where φ is a smoothing or sensitivity parameter, such that $0 < \varphi \leq 1$. The starting value of X_t is assumed to be $k\theta_0$, i.e., $X_0 = k\theta_0$. The mean and variance of X_t for the IC process, respectively, are given as follows:

$$E(X_t) = k\theta_0, \text{ and } \text{Var}(X_t) = \frac{\varphi}{2-\varphi} \{1 - (1 - \varphi)^{2t}\} k\theta_0^2. \quad (3)$$

To detect the two-sided changes in the process, the control limits UCL_t and LCL_t for the two-sided EWMA TBE chart are given as follows:

$$\left. \begin{aligned} UCL_t &= k\theta_0 + L \sqrt{\frac{\varphi}{2-\varphi} \{1 - (1-\varphi)^{2t}\} k\theta_0^2}, \\ LCL_t &= \max \left(0, k\theta_0 - L \sqrt{\frac{\varphi}{2-\varphi} \{1 - (1-\varphi)^{2t}\} k\theta_0^2} \right). \end{aligned} \right\} \quad (4)$$

where L denotes the width coefficient for the EWMA TBE chart. The two-sided EWMA TBE chart and statistic X_t is plotted versus time t , and the process is declared to be OOC if $X_t \geq UCL_t$ or $X_t \leq LCL_t$; otherwise, the process is declared to be IC.

2.3. DEWMA TBE chart

The DEWMA TBE chart introduced by Alevizakos and Koukouvinos [11], can be defined by the plotting statistic Y_t , defined as follows:

$$Y_t = \varphi X_t + (1-\varphi)Y_{t-1}, \quad t = 1, 2, \dots, \quad (5)$$

where the starting value $Y_0 = k\theta_0$. Based on Eq (5), the mean and variance of Z_t for the IC process, respectively, are defined as follows:

$$E(Y_t) = k\theta_0, \text{ and } Var(Y_t) = \frac{\varphi^4 [1+(1-\varphi)^2-(t+1)^2(1-\varphi)^{2t}+(2t^2+t-1)(1-\varphi)^{2t+2}-t^2(1-\varphi)^{2t+4}] k\theta_0^2}{[1-(1-\varphi)^2]^3}. \quad (6)$$

Based on $E(Y_t)$ and $Var(Y_t)$, the two-sided DEWMA TBE chart control limits UCL_t and LCL_t are given as follows:

$$\left. \begin{aligned} UCL_t &= k\theta_0 + L \sqrt{\frac{\varphi^4 [1+(1-\varphi)^2-(t+1)^2(1-\varphi)^{2t}+(2t^2+t-1)(1-\varphi)^{2t+2}-t^2(1-\varphi)^{2t+4}] k\theta_0^2}{[1-(1-\varphi)^2]^3} k\theta_0^2}, \\ LCL_t &= \max \left(0, k\theta_0 - L \sqrt{\frac{\varphi^4 [1+(1-\varphi)^2-(t+1)^2(1-\varphi)^{2t}+(2t^2+t-1)(1-\varphi)^{2t+2}-t^2(1-\varphi)^{2t+4}] k\theta_0^2}{[1-(1-\varphi)^2]^3} k\theta_0^2} \right). \end{aligned} \right\} \quad (7)$$

To monitor the decreasing or increasing shifts in the process, the two-sided DEWMA TBE chart is constructed by plotting the statistic Y_t against time t and if $Y_t \geq UCL_t$ or $Y_t \leq LCL_t$, then the process is deemed to be OOC; otherwise, the process is considered to be IC.

2.4. TEWMA TBE chart

Alevizakos et al. [12] proposed the TEWMA TBE chart, which has the charting statistic Z_t , defined as follows:

$$Z_t = \varphi Y_t + (1-\varphi)Z_{t-1}, \quad t = 1, 2, \dots \quad (8)$$

The initial value of Z_t is equal to $k\theta_0$, i.e., $Z_0 = k\theta_0$. The IC mean of the statistic Z_t is $E(Z_t) = k\theta_0$, while its variance is given as follows:

$$\begin{aligned} Var(Z_t) &= \left[\frac{\tau^3 \varphi^6}{4} \left\{ -\frac{t(t^2-1)(t-2)\tau^{t-3}}{1-\tau} - \frac{4t(t^2-1)\tau^{t-2}}{(1-\tau)^2} - \frac{12t(t+1)\tau^{t-1}}{(1-\tau)^3} - \frac{24(t+1)\tau^t}{(1-\tau)^4} + \frac{24(1-\tau^{t+1})}{(1-\tau)^5} \right\} + \right. \\ &\quad \left. 2\tau^2 \varphi^6 \left\{ -\frac{t(t^2-1)\tau^{t-2}}{1-\tau} - \frac{3t(t+1)\tau^{t-1}}{(1-\tau)^2} - \frac{6(t+1)\tau^t}{(1-\tau)^3} + \frac{6(1-\tau^{t+1})}{(1-\tau)^4} \right\} + \frac{7\tau\varphi^6}{2} \left\{ -\frac{t(t+1)\tau^{t-1}}{1-\tau} - \frac{2(t+1)\tau^t}{(1-\tau)^2} + \right. \right. \end{aligned}$$

$$\frac{2(1-\tau^{t+1})}{(1-\tau)^3} + \varphi^6 \left\{ \frac{1-\tau^{t+1}}{(1-\tau)^2} - \frac{(t+1)\tau^t}{1-\tau} \right\} k\theta_0^2. \quad (9)$$

where $\tau = (1 - \varphi)^2$. To detect the decreasing or increasing changes in the process, via TEWMA TBE chart, the control limits, i.e., UCL_t and LCL_t are defined as follows:

$$\begin{aligned} UCL_t &= k\theta_0 + L\sqrt{Var(Z_t)}, \\ LCL_t &= \max(0, k\theta_0 - L\sqrt{Var(Z_t)}). \end{aligned} \quad (10)$$

In this case, the TEWMA TBE statistic Z_t is plotted versus time t , and if $Z_t \geq UCL_t$ or $Z_t \leq LCL_t$ then the process is regarded as OOC; otherwise, the process is considered to be IC.

2.5. HWMA TBE chart

The HWMA chart for TBE introduced by Aslam et al. [3] is referred to as the HWMA TBE chart. Let U_t be the charting statistic, then it can be defined as follows:

$$U_t = \varphi T_t + (1 - \varphi) \bar{T}_{t-1}, \quad t = 1, 2, \dots, \quad (11)$$

where $\bar{T}_{t-1} = \frac{\sum_{j=1}^{t-1} T_j}{t-1}$ is the mean of previous $t - 1$ observations. The starting values U_0 and \bar{T}_0 are set to $k\theta_0$, i.e., $U_0 = \bar{T}_0 = k\theta_0$. The IC mean and variance of U_t (cf. Appendices A, and B) are provided as follows:

$$E(U_t) = k\theta_0, \quad Var(U_t) = \varphi^2 k\theta_0^2, \text{ if } t = 1, \text{ and } Var(U_t) = \left\{ \varphi^2 + \frac{(1-\varphi)^2}{t-1} \right\} k\theta_0^2, \text{ if } t > 1. \quad (12)$$

The two-sided HWMA TBE chart control limits, i.e., UCL_t and LCL_t can be given as follows:

$$\begin{aligned} UCL_t &= \begin{cases} k\theta_0 + L\sqrt{\varphi^2 k\theta_0^2} & \text{if } t = 1, \\ k\theta_0 + L\sqrt{\left\{ \varphi^2 + \frac{(1-\varphi)^2}{t-1} \right\} k\theta_0^2} & \text{if } t > 1, \end{cases} \\ LCL_t &= \begin{cases} \max(0, k\theta_0 - L\sqrt{\varphi^2 k\theta_0^2}) & \text{if } t = 1, \\ \max(0, k\theta_0 - L\sqrt{\left\{ \varphi^2 + \frac{(1-\varphi)^2}{t-1} \right\} k\theta_0^2}) & \text{if } t > 1. \end{cases} \end{aligned} \quad (13)$$

For monitoring the downward or upward shifts in the process, the two-sided HWMA TBE chart is formulated and the statistic U_t is plotted versus time t . Whenever $U_t \geq UCL_t$ or $U_t \leq LCL_t$, the process is considered to be OOC; otherwise, the process is deemed to be IC.

2.6. DHWMA TBE chart

The gamma distribution-based DHWMA charts for monitoring TBE may be referred to as the DHWMA TBE charts. The DHWMA TBE statistic is symbolized by V_t , and is defined as follows:

$$V_t = \varphi U_t + (1 - \varphi) \bar{T}_{t-1}, \quad t = 1, 2, \dots \quad (14)$$

The starting value of the statistic V_t is equal to the IC TBE mean, i.e., $V_0 = k\theta_0$. The IC process

mean and variance of the statistic V_t , (cf. Appendices A, B and C), are given as follows:

$$E(V_t) = k\theta_0, \text{Var}(V_t) = \varphi^4 k\theta_0^2, \text{ if } t = 1, \text{ and } \text{Var}(V_t) = \left\{ \varphi^4 + \frac{(1-\varphi^2)^2}{t-1} \right\} k\theta_0^2, \text{ if } t > 1. \quad (15)$$

The control limits UCL_t and LCL_t of the two-sided DHWMA TBE chart to identify the downward or upward shifts, are given as follows:

$$\begin{aligned} UCL_t &= \begin{cases} k\theta_0 + L\sqrt{\varphi^4 k\theta_0^2} & \text{if } t = 1, \\ k\theta_0 + L\sqrt{\left\{ \varphi^4 + \frac{(1-\varphi^2)^2}{t-1} \right\} k\theta_0^2} & \text{if } t > 1. \end{cases} \\ LCL_t &= \begin{cases} \max(0, k\theta_0 - L\sqrt{\varphi^4 k\theta_0^2}) & \text{if } t = 1, \\ \max(0, k\theta_0 - L\sqrt{\left\{ \varphi^4 + \frac{(1-\varphi^2)^2}{t-1} \right\} k\theta_0^2}) & \text{if } t > 1. \end{cases} \end{aligned} \quad (16)$$

The statistic V_t is plotted against time t , and the process is said to be OOC if $V_t \geq UCL_t$ or $V_t \leq LCL_t$; otherwise, the process is said to be IC.

2.7. THWMA TBE chart

Riaz et al. [17] designed the THEMA chart for monitoring the mean level of the process. The methodology of the THWMA chart can be extended to design the develop one- and two-sided THWMA charts to monitor the gamma-distributed *TBE* observations. The proposed charts are called the THWMA TBE charts. If W_t is the charting statistic for the THWMA TBE chart, then it can be expressed by linear equations, defined as follows:

$$W_t = \varphi V_t + (1 - \varphi) \bar{T}_{t-1}, t = 1, 2, \dots, \quad (17)$$

with starting value $W_0 = k\theta_0$. The IC mean and variance of the statistic W_t , (cf. Appendices A, B, C and D) are given as follows:

$$E(W_t) = k\theta_0, \text{Var}(W_t) = \varphi^6 k\theta_0^2, \text{ if } t = 1, \text{ and } \text{Var}(W_t) = \left\{ \varphi^6 + \frac{(1-\varphi^3)^2}{t-1} \right\} k\theta_0^2, \text{ if } t > 1. \quad (18)$$

To identify the decrease in interarrival time, the limit LCL_t of the lower-sided THWMA TBE chart is defined as follows:

$$LCL_t = \begin{cases} k\theta_0 - L\sqrt{\varphi^6 k\theta_0^2} & \text{if } t = 1, \\ k\theta_0 - L\sqrt{\left\{ \varphi^6 + \frac{(1-\varphi^3)^2}{t-1} \right\} k\theta_0^2} & \text{if } t > 1. \end{cases} \quad (19)$$

The statistic W_t is plotted against time t , and if $W_t \leq LCL_t$, the THWMA TBE chart states the process is OOC; otherwise, the process is IC. Similarly, to monitor the increase in interarrival time, the limit UCL_t of the upper-sided THWMA TBE chart is given as follows:

$$UCL_t = \begin{cases} k\theta_0 + L\sqrt{\varphi^6 k\theta_0^2} & \text{if } t = 1, \\ k\theta_0 + L\sqrt{\left\{\varphi^6 + \frac{(1-\varphi^3)^2}{t-1}\right\} k\theta_0^2} & \text{if } t > 1. \end{cases} \quad (20)$$

The charting statistic W_t is plotted against time t , and if $W_t \geq UCL_t$ the process under the THWMA TBE chart is OOC; otherwise, the process is IC. Likewise, to monitor the decrease or increase in interarrival time, the two-sided THWMA TBE chart control limits, i.e., UCL_t and LCL_t , are presented as follows:

$$\begin{aligned} UCL_t &= \begin{cases} k\theta_0 + L\sqrt{\varphi^6 k\theta_0^2} & \text{if } t = 1, \\ k\theta_0 + L\sqrt{\left\{\varphi^6 + \frac{(1-\varphi^3)^2}{t-1}\right\} k\theta_0^2} & \text{if } t > 1. \end{cases} \\ LCL_t &= \begin{cases} \max(0, k\theta_0 - L\sqrt{\varphi^6 k\theta_0^2}) & \text{if } t = 1, \\ \max\left(0, k\theta_0 - L\sqrt{\left\{\varphi^6 + \frac{(1-\varphi^3)^2}{t-1}\right\} k\theta_0^2}\right) & \text{if } t > 1. \end{cases} \end{aligned} \quad (21)$$

In this case, the charting statistic W_t is plotted against t , and the process under the two-sided THWMA TBE chart is considered to be OOC when $W_t \geq UCL_t$ or $W_t \leq LCL_t$; otherwise, the process is deemed to be IC.

3. Design and implementation of THWMA TBE chart

The design structure of the THWMA TBE chart is based on the smoothing parameters φ and chart width L . The combinations of φ and L are chosen so that the ARL_0 is close to the desired value. The ARL_0 is set to 370 in this study. Furthermore, THWMA TBE charts are used with time-varying control limits.

3.1. Performance evaluation measures

The performance of the chart is often evaluated using run-length metrics such as ARL, SDRL, percentile points, etc. The ARL is referred to as the average number of sample points depicted on the chart until a point reveals an OOC signal [23]. ARLs are classified into two types: IC ARL (ARL_0) and OOC ARL (ARL_1). When a process is operating in an IC state, then the ARL_0 is anticipated to be large enough in order to avert false alarms, whereas when a process is functioning in an OOC state, then ARL_1 should remain small to identify the process change quickly [24]. To compare the efficiency of two or more charts, it is advisable to set the common ARL_0 for these charts. For a particular shift, the chart with the smaller ARL_1 value is deemed to be sensitive and may detect a specific shift faster than the other charts.

3.2. Overall performance measures

The ARL measures assess the performance of the chart for a single specified shift in the process parameters. Extra quadratic loss (EQL), relative average run length (RARL) and performance comparison index (PCI) are additional performance measures that evaluate a chart's overall

performance over a certain range of shifts.

The EQL is the weighted ARL over the range of shifts, i.e., δ_{min} to δ_{max} , using the square of the shift as a weight [25]. Mathematically, EQL can be defined as follows:

$$EQL = \frac{1}{\delta_{max} - \delta_{min}} \int_{\delta_{min}}^{\delta_{max}} \delta^2 ARL(\delta) d\delta, \quad (22)$$

where $ARL(\delta)$ is the ARL of a particular chart at a shift δ . A chart with a lower EQL value is regarded as more efficient.

The RARL is referred to as the ratio of the ARL of a certain chart, i.e., $ARL(\delta)$ to the ARL benchmark chart, i.e., $ARL_{bmk}(\delta)$ [26]. The RARL may be defined mathematically, as follows:

$$RARL = \frac{1}{\delta_{max} - \delta_{min}} \int_{\delta_{min}}^{\delta_{max}} \frac{ARL(\delta)}{ARL_{bmk}(\delta)} d\delta. \quad (23)$$

A benchmark chart might be considered as a chart with a minimum EQL or as one of the current standard charts.

According to Ou et al. [27], PCI is defined as the ratio of a chart's EQL to the EQL of the benchmark chart. It is mathematically given as follows:

$$PCI = \frac{EQL}{EQL_{bmk}}. \quad (24)$$

The PCI value is equal to one for the benchmark chart and it is more than one for the other charts.

3.3. Implementation of THWMA TBE chart

To implement the THWMA TBE chart, a simulation study is carried out. A computational methodology of Monte Carlo simulations is used as the design structure of the THWMA TBE chart and is more complicated than that of other charts. Furthermore, when time-varying control limits are considered, computational techniques such as the Markov chain and integral equations have been used limitedly.

To execute the simulation study, various combinations of $k = 1, 2, 3$ and $\varphi = 0.05, 0.1, 0.2$ are used to compute the chart coefficients values, i.e., L , so that ARL_0 is close to 370. For the sake of convenience, if the process is IC, then it is assumed that $\theta = \theta_0 = 1$; however, if the process is OOC, then $\theta = \theta_1 = \delta\theta_0$, where $\delta = 0.975, 0.95, 0.925, 0.9, 0.85, 0.8, 0.7, 0.5, 0.25$ for the downward changes and $\delta = 1.025, 1.05, 1.08, 1.11, 1.18, 1.25, 1.43, 2.4$ for upward shifts. A simulation algorithm is developed in R software and can be described in the steps given as follows:

- (i) Generate T_t from gamma (k, θ) , i.e., $T_t \sim \text{gamma}(k, \theta_0), t = 1, 2, \dots$ for each $k = 1, 2, 3$.
- (ii) Compute the statistic U_t from Eq (11) using T_t .
- (iii) Using the statistic U_t as input, compute the statistic V_t in Eq (14).
- (iv) Using the statistic V_t as input, compute the THWMA TBE statistic W_t in Eq (17).
- (v) Choose the design parameters (φ, L) for the desired ARL_0 .
- (vi) Calculate UCL_t and LCL_t in Eq (21) based on L and φ .
- (vii) Plot the THWMA TBE statistic W_t along UCL_t and LCL_t .
- (viii) When $W_t \geq UCL_t$ or $W_t \leq LCL_t$, the sequence order called run length (RL) is recorded.
- (ix) Replicate steps (i)-(viii) 10^6 times and record RLs.

- (x) Calculate the average and standard deviation of 10^6 RL, i.e., ARL_0 and $SDRL_0$. Check whether the calculated ARL_0 is the desired ARL_0 ; otherwise, adjust L and repeat steps (i)-(ix) until the desired ARL_0 is achieved.
- (xi) Compute ARL_1 and $SDRL_1$ (OOC SDRL) values by considering $T_t \sim \text{gamma}(k, \theta_1)$, $t = 1, 2, 3, \dots$, where $\theta_1 = \delta\theta_0$ with $\delta \neq 1$ and replicate steps (ii)-(ix).

It should be noted that the ARL and SDRL values may be determined using their respective expressions, which are given as follows:

$$ARL = \frac{\sum_{t=1}^N RL_t}{N}, \quad (25)$$

$$SDRL = \sqrt{\frac{\sum_{t=1}^N (RL_t - ARL)^2}{N-1}}. \quad (26)$$

where N is the number of simulation runs, which is specified to be in this study as $N = 10^6$.

The above simulation algorithm is developed to compute the ARL and SDRL values for the two-sided THWMA TBE chart. However, to calculate the ARL and SDRL values for the one-sided chart, the control limit is specified in Eqs (19) and (20) are, respectively, required for lower- and upper-sided THWMA TBE charts. Moreover, a similar algorithm can also be used to determine the ARL and SDRL findings for the competing charts. The simulation results, i.e., the ARL and SDRL (specified in the parenthesis) values for the THWMA TBE charts, along with the competing charts, are shown in Tables 1–6. For each shift, the smallest ARL_1 values are shown in bold print.

4. Performance and comparative study

This section covers the performance and comparative study for the THWMA TBE charts. The THWMA TBE charts are compared to competing charts, including the DHWMA TBE, HWMA TBE, TEWMA TBE, DEWMA TBE and EWMA TBE charts. Details of the performance and comparative analysis are as follows:

From Tables 1–6, it can be concluded that for a given value of φ , the performance behavior of the THWMA TBE charts is enhanced as the value of k rises. For example, if $\varphi = 0.05$ and $\delta = 0.95$, then the lower-sided THWMA TBE chart provides $ARL_1 = 22.7$ when $k = 1$, while it yields $ARL_1 = 15.63$ when $k = 2$ and it has $ARL_1 = 12.93$ when $k = 3$. A similar type of behavior can be observed with the upper- and two-sided THWMA TBE charts. In addition, for a specified k , the performance behavior of the two-sided THWMA TBE chart worsens when the values of φ increase. For instance, when $k = 1$ and $\delta = 0.9$, then the two-sided THWMA TBE chart achieves $ARL_1 = 40.01$ with $\varphi = 0.05$, whereas it holds $ARL_1 = 48.88$ with $\varphi = 0.1$, and it receives $ARL_1 = 123.12$ with $\varphi = 0.2$. Similarly, for $k = 1, 2$. The performance of the upper-sided THWMA TBE chart deteriorates with increasing values of φ . For instance, at $k = 1$ and $\delta = 1.025$, for $\varphi = 0.05$ the upper-sided THWMA TBE chart has $ARL_1 = 54.62$, for $\varphi = 0.1$, it has $ARL_1 = 59.52$ and for $\varphi = 0.2$, it has $ARL_1 = 185.03$. However, this is not observed for the lower-sided THWMA TBE chart with any k . For instance, when $k = 2$ and $\delta = 0.925$, the lower-sided THWMA TBE chart has $ARL_1 = 8.24$ if $\varphi = 0.05$, $ARL_1 = 8.02$ if $\varphi = 0.1$ and $ARL_1 = 12.58$ if $\varphi = 0.2$. Furthermore, for a given value of k and φ , the lower-sided THWMA TBE chart has better detection ability than the upper-sided THWMA TBE chart. For example, if $k = 3$ and $\varphi = 0.1$, the lower-sided THWMA TBE chart has $ARL_1 = 12.61$ when $\delta = 0.95$ (1.05 time less than θ_0), whereas the upper-sided

THWMA TBE chart has $ARL_1 = 15.15$ when $\delta = 1.05$ (1.05 time greater than θ_0). Also, for $k = 1$, the two-sided THWMA TBE chart is just ARL -biased for very small downward shifts, i.e., $0.975 \leq \delta < 1$ when $\varphi = 0.2$. Moreover, as far as the SDRL values are concerned, it can be observed that when the value of φ rises, the IC SDRL ($SDRL_0$) values reduce. For example, when $k = 3$, then the two-sided THWMA TBE chart has $SDRL_0 = 3368.86$ when $\varphi = 0.05$, though the two-sided THWMA TBE chart has $SDRL_0 = 2444.97$ when $\varphi = 0.1$ and the two-sided THWMA TBE chart has $SDRL_0 = 677.96$ when $\varphi = 0.2$. Similar inferences may be drawn for the one-sided THWMA TBE charts. It should be noted that the results regarding the competing charts, i.e., the DHWMA TBE, HWMA TBE, TEWMA TBE, DEWMA TBE, and EWMA TBE charts, those observed along with the THWMA TBE chart can be discussed in the same manner.

In comparing the THWMA TBE charts against the competing TBE charts, it is observed that the THWMA TBE charts gain excellent performance against the corresponding EWMA TBE charts for small and large shifts. For example, if $k = 1$, $\varphi = 0.1$ and $\delta = 0.975, 0.95, \dots, 0.25$, then the lower-sided THWMA TBE chart has $ARL_1 = 48.61, 21.54, \dots, 1.11$, while the lower-sided EWMA TBE has $ARL_1 = 296.22, 237.58, \dots, 7.22$. The THWMA TBE charts reveal superior performance over the DHWMA TBE charts for every shift value. For instance, when $k = 2$, $\varphi = 0.05$ and $\delta = 1.025, 1.05, \dots, 4$, the upper-sided THWMA TBE chart has $ARL_1 = 37.41, 18.15, \dots, 1.22$, whereas the upper-sided DHWMA TBE has $ARL_1 = 225.87, 148.84, \dots, 1.48$. The THWMA TBE charts show better detection ability relative to the TEWMA TBE charts for each shift value. For example, when $k = 3$, $\varphi = 0.05$ and $\delta = 0.25, 0.5, \dots, 4$, the two-sided THWMA TBE chart has $ARL_1 = 4.06, 6.90, \dots, 2.26$, but the upper-sided DHWMA TBE has $ARL_1 = 8.51, 18.46, \dots, 2.77$. The THWMA TBE charts achieve better detection ability over the TEWMA TBE charts for each shift value. For example, when $k = 3$, $\varphi = 0.05$ and $\delta = 0.25, 0.5, \dots, 4$, the two-sided THWMA TBE chart has $ARL_1 = 4.06, 6.90, \dots, 2.26$, where the upper-sided DHWMA TBE has $ARL_1 = 8.51, 18.46, \dots, 2.77$. The THWMA TBE charts have better performance compared with the respective HWMA TBE charts for every single shift. For instance, if $k = 1$, $\varphi = 0.2$ and $\delta = 0.975, 0.95, \dots, 0.25$, then the lower-sided THWMA TBE chart has $ARL_1 = 58.14, 27.88, \dots, 1.17$; however, the upper-sided HWMA TBE has $ARL_1 = 105.69, 58.09, \dots, 2.43$. The THWMA TBE charts have better performance compared with the DHWMA TBE charts for every shift. For example, when $k = 2$, $\varphi = 0.1$ and $\delta = 0.25, 0.5, \dots, 4$, the ARL_1 values of the two-sided THWMA TBE chart are $4.57, 8.66, \dots, 1.58$, on the other hand, the ARL_1 values the upper-sided DHWMA TBE are $6.85, 14.96, \dots, 1.72$. Similar types of conclusions can also be drawn from the ARL plots of the one- and two-sided THWMA TBE versus one- and two-sided competing charts, given in the Figures 1 to 3.

The overall comparisons of the THWMA TBE charts against the rival *TBE* charts indicate that the THWMA TBE charts show better overall performance as compared to the EWMA TBE charts in term of minimum *EQL*, *RARL* and *PCI* values. For example, when $k = 1$ and $\varphi = 0.05$, then the upper-sided THWMA TBE chart has $EQL = 17.35$, $RARL = 1.00$ and $PCI = 1.00$, whereas the upper-sided EWMA TBE chart has $EQL = 47.59$, $RARL = 2.74$ and $PCI = 3.35$. The THWMA TBE charts demonstrate superior overall performance relative to the DEWMA TBE charts. For instance, when $k = 2$ and $\varphi = 0.1$, the lower-sided THWMA TBE chart has $EQL = 9.08$, $RARL = 1.00$ and $PCI = 1.00$; whereas, the upper-sided DHWMA TBE chart has $EQL = 34.68$, $RARL = 3.82$ and $PCI = 7.53$. The THWMA TBE charts reveal an improved overall performance against the TEWMA TBE charts. For instance, if $k = 3$ and $\varphi = 0.05$, then the two-sided THWMA TBE chart has $EQL = 16.35$, $RARL = 1.00$ and $PCI = 1.00$, where the two-sided TEWMA TBE chart has

$EQL = 30.33$, $RARL = 1.86$ and $PCI = 1.88$. The THWMA TBE charts indicate dominant overall performance against the HWMA TBE charts. For instance, when $k = 2$ and $\varphi = 0.2$, the lower-sided THWMA TBE chart has $EQL = 10.35$, $RARL = 1.00$ and $PCI = 1.00$, but the lower-sided HWMA TBE chart has $EQL = 18.19$, $RARL = 1.76$ and $PCI = 2.76$. The THWMA TBE charts have enhanced overall performance as compared to the DHWMA TBE charts. For example, for $k = 1$ and $\varphi = 0.1$, the lower-sided THWMA TBE chart has $EQL = 10.35$, $RARL = 1.00$ and $PCI = 1.00$; in contrast, the lower-sided DHWMA TBE chart has $EQL = 18.19$, $RARL = 1.76$ and $PCI = 2.76$.

Table 1. ARL and SDRL values for the one-sided THWMA TBE chart and one-sided competing charts when $k = 1$ and $ARL_0 \cong 370$.

THWMA TBE			DHWMA TBE			HWMA TBE			TEWMA TBE			DEWMA TBE			EWMA TBE			
$\varphi =$	0.1	0.2	0.05	0.1	0.2	0.05	0.1	0.2	0.05	0.1	0.2	0.05	0.1	0.2	0.05	0.1	0.2	
δ	L =	0.26	0.36	0.27	0.40	0.72	0.77	0.89	0.95	1.24	1.54	1.77	1.45	1.72	1.87	1.86	1.90	1.81
	0.272	6	5	9	7	7	5	37	57	7	65	8	2	24	4	97	3	
1	370.7	370.	370.	370.	370.	369.	369.	369.	370.	370.	370.	370.	369.	370.	370.	370.	370.	
	5	94	47	61	72	59	89	04	33	79	38	13	24	38	64	19	29	32
	(3815)	(373)	(317)	(365)	(299)	(180)	(173)	(166)	(177)	(411)	(374)	(365)	(396)	(369)	(365)	(371)	(366)	(365)
	.50)	9.56)	4.29)	2.89)	2.97)	4.33)	0.96)	7.67)	7.22)	.21)	.71)	.78)	.92)	.53)	.48)	.28)	.80)	.86)
0.9	49.03	48.6	58.1	49.1	63.8	102.	106.	110.	105.	261.	278.	295.	264.	282.	301.	279.	296.	312.
75	1	4	5	7	78	97	23	69	35	88	66	61	72	34	50	22	23	
	(328.)	(323.)	(296.)	(307.)	(303.)	(325.)	(324.)	(314.)	(312.)	(287)	(280)	(289)	(280)	(279)	(296)	(277)	(289)	(307)
	91)	89)	60)	98)	60)	42)	43)	11)	94)	.31)	.62)	.27)	.45)	.94)	.07)	.63)	.72)	.18)
0.9	22.07	21.5	27.8	22.2	30.2	54.9	57.7	60.9	58.0	188.	212.	237.	194.	220.	246.	213.	237.	262.
5	4	8	9	6	2	5	0	9	61	24	56	57	00	28	82	58	98	
	(105.)	(102.)	(115.)	(106.)	(119.)	(144.)	(143.)	(139.)	(136.)	(203)	(210)	(230)	(200)	(216)	(240)	(208)	(230)	(255)
	27)	71)	68)	93)	27)	50)	98)	07)	41)	.17)	.35)	.09)	.97)	.67)	.30)	.45)	.15)	.52)
0.9	13.81	13.5	17.3	14.1	19.4	35.6	38.3	41.5	39.3	141.	164.	191.	147.	173.	202.	167.	192.	222.
25	4	1	5	0	7	1	8	7	50	29	86	64	60	15	47	26	08	
	(54.9)	(54.1)	(61.5)	(56.3)	(65.9)	(82.9)	(84.2)	(82.7)	(79.0)	(148)	(160)	(184)	(150)	(168)	(196)	(160)	(184)	(215)
	3)	3)	2)	9)	6)	1)	5)	8)	4)	.27)	.24)	.79)	.71)	.07)	.46)	.18)	.79)	.06)
0.9	9.82	9.90	12.4	10.4	13.6	26.2	27.8	30.6	29.3	108.	129.	156.	114.	137.	166.	131.	156.	186.
	9)	0	9	0	8	1	1	30	44	75	17	19	74	85	81	59		
	(33.1)	(33.7)	(38.7)	(34.9)	(41.0)	(55.6)	(55.9)	(55.2)	(52.4)	(110)	(122)	(149)	(114)	(130)	(158)	(123)	(148)	(180)
	5)	6)	7)	9)	9)	7)	8)	5)	8)	.50)	.41)	.43)	.02)	.01)	.84)	.61)	.87)	.44)
0.8	6.19	6.18	7.67	6.36	8.34	15.8	17.4	19.5	18.9	69.0	83.8	105.	72.4	89.6	114.	86.3	105.	134.
5				8		0	5	7	4	5	19	7	7	14	5	48	26	
	(15.9)	(16.1)	(19.1)	(16.5)	(20.3)	(29.3)	(30.4)	(29.9)	(28.4)	(66.)	(74.)	(96.)	(67.)	(81.)	(106)	(76.)	(96.)	(127)
	7)	5)	1)	2)	3)	7)	4)	6)	5)	.08)	.61)	.89)	.79)	.37)	.82)	.56)	.36)	.21)
0.8	4.52	4.49	5.43	4.68	5.93	11.0	12.0	13.7	13.6	47.4	57.8	73.1	48.9	61.6	80.3	59.0	73.6	96.9
				9		4	8	1	8	8	8	4	8	9	9	4	9	

Continued on next page

		(9.78)	(9.66)	(11.4)	(10.2)	(12.3)	(18.2)	(18.5)	(18.7)	(17.6)	(42.)	(47.)	(64.)	(43.)	(52.)	(72.)	(48.)	(64.)	(89.)
0.7	2.95	2.93	3.40		3.02	3.61	6.49	7.06	8.28	8.33	26.0	31.8	38.4	26.7	32.8	42.1	32.4	39.1	51.9
		(4.52)	(4.53)	(5.25)	(4.73)	(5.53)	(8.62)	(8.98)	(9.20)	(8.62)	(21.)	(22.)	(29.)	(20.)	(23.)	(34.)	(22.)	(29.)	(44.)
0.5	1.74	1.73	1.92		1.75	2.01	3.19	3.45	4.14	4.31	10.6	13.7	15.2	11.0	13.6	15.6	13.9	15.5	18.1
		(1.64)	(1.62)	(1.85)	(1.66)	(1.94)	(2.84)	(2.97)	(3.14)	(3.00)	(7.3)	(7.1)	(7.5)	(6.5)	(6.8)	(8.5)	(6.6)	(7.9)	(11.)
0.2	1.11	1.10	1.17		1.12	1.20	1.72	1.86	2.27	2.43	4.53	6.50	7.43	5.01	6.51	7.08	6.76	7.22	7.25
5		(0.50)	(0.49)	(0.59)	(0.51)	(0.64)	(1.09)	(1.14)	(1.15)	(0.99)	(1.8)	(1.9)	(1.7)	(1.6)	(1.7)	(1.7)	(1.6)	(1.7)	(2.1)
))))))))	7)	8)	8)	6)	2)	2)	6)	8)	8)
<i>EQL</i>		10.24	10.1	11.0	10.2	11.5	15.5	16.0	16.8	16.5	38.3	43.2	49.2	39.3	44.8	51.6	43.8	49.4	57.0
<i>RARI</i>		7	6	7	2	2	9	7	3	2	9	4	6	2	7	1	1	7	
<i>PCI</i>		1.00	1.00	1.00	1.00	1.13	1.40	1.57	1.66	1.49	3.74	4.26	4.45	3.85	4.41	4.67	4.28	4.86	5.16
		1.00	1.00	1.00	1.02	1.22	1.78	2.21	2.59	2.27	7.44	9.33	9.43	7.75	9.60	9.94	9.44	11.0	11.5
																	8	6	
$\varphi =$		0.05	0.1	0.2	0.05	0.1	0.2	0.05	0.1	0.2	0.05	0.1	0.2	0.05	0.1	0.2	0.05	0.1	0.2
$L =$		0.089	0.13	0.87	0.37	1.02	2.60	2.98	4.02	4.60	1.31	1.75	2.25	1.57	2.02	2.54	2.46	2.93	3.49
δ		5	1	8	7	4	8	3	3	1	3	9	8	2	1	8	1	5	8
1		370.4	370.	370.	370.	370.	370.	370.	370.	369.	369.	370.	369.	370.	370.	369.	370.	370.	
		3	20	70	72	39	02	67	34	00	73	99	29	55	78	27	68	33	94
		(3629)	(287)	(739.)	(156)	(640.)	(282.)	(265.)	(273.)	(320.)	(435)	(404)	(386)	(425)	(399)	(383)	(398)	(383)	(375)
		.03)	9.28)	58)	5.41)	23)	30)	69)	91)	31)	92)	.70)	.18)	.14)	.15)	.93)	.42)	.86)	.63)
1.0		54.62	59.5	185.	104.	200.	283.	289.	299.	303.	253.	269.	282.	258.	273.	289.	270.	284.	298.
25		2	03	23	93	24	72	61	53	00	89	16	37	17	81	56	64	52	
		(322.)	(305.)	(366.)	(381.)	(347.)	(215.)	(206.)	(218.)	(261.)	(296)	(293)	(295)	(296)	(294)	(299)	(293)	(296)	(302)
		76)	20)	21)	58)	10)	45)	22)	64)	52)	.01)	.58)	.59)	.34)	.88)	.29)	.22)	.16)	.19)
1.0		26.32	30.4	110.	53.3	126.	222.	232.	248.	255.	184.	202.	221.	188.	207.	227.	204.	223.	243.
5		2	58	7	11	73	43	00	87	11	94	63	02	12	69	66	95	73	
		(107.)	(120.)	(216.)	(172.)	(217.)	(171.)	(165.)	(177.)	(216.)	(213)	(220)	(231)	(215)	(223)	(236)	(221)	(232)	(246)
		20)	79)	51)	24)	45)	23)	67)	14)	91)	.37)	.48)	.40)	.37)	.58)	.28)	.38)	.08)	.53)
1.0		16.89	19.0	68.4	32.0	80.3	172.	183.	200.	207.	132.	150.	168.	135.	154.	176.	151.	172.	194.
8		0	2	3	4	19	14	52	91	12	49	79	42	15	19	36	27	53	
		(55.1)	(62.0)	(130.)	(89.8)	(138.)	(132.)	(129.)	(139.)	(172.)	(152)	(162)	(175)	(154)	(165)	(183)	(162)	(177)	(196)
		2)	5)	75)	8)	24)	57)	75)	30)	46)	.00)	.01)	.79)	.10)	.47)	.26)	.65)	.63)	.56)
1.1		12.83	13.7	47.7	21.9	56.6	137.	148.	166.	174.	100.	114.	133.	102.	119.	139.	116.	135.	157.
1		0	1	6	6	48	75	95	48	21	70	24	14	19	15	05	25	42	

Continued on next page

	(36.1	(37.8	(89.4	(56.0	(96.0	(107.	(106.	(114.	(143.	(112	(121	(138	(115	(127	(143	(124	(139	(159	
	0)	5)	9)	6)	2)	68)	25)	98)	98)	.69)	.54)	.27)	.41)	.21)	.68)	.59)	.93)	.74)	
1.1	8.19	8.81	26.0	12.8	30.8	87.7	97.7	114.	120.	60.1	69.2	82.4	60.2	72.2	86.6	69.3	84.3	103.	
8			2	9	2	7	5	13	03	3	4	3	2	0	2	6	3	42	
	(17.8	(19.1	(45.0	(26.6	(50.1	(70.9	(71.1	(76.8	(95.5	(66.	(71.	(84.	(66.	(75.	(89.	(73.	(87.	(103	
	7)	6)	4)	5)	6)	1)	4)	8)	3)	03)	93)	12)	59)	81)	20)	46)	25)	.95)	
1.2	6.31	6.72	16.9	9.27	19.9	60.6	69.0	83.3	87.6	41.3	47.5	55.4	40.2	48.4	58.8	46.8	57.6	71.5	
5			8	7	2	6	1	2	3	6	3	5	4	8	1	0	0		
	(11.4	(12.4	(27.4	(16.6	(30.9	(50.8	(52.0	(55.8	(68.4	(44.	(47.	(55.	(43.	(50.	(60.	(49.	(58.	(71.	
	8)	2)	9)	3)	4)	0)	8)	8)	4)	35)	96)	72)	85)	16)	16)	28)	41)	88)	
1.4	4.20	4.37	9.02	5.66	10.2	30.3	35.3	45.2	47.0	21.3	24.2	27.6	20.1	23.6	28.4	22.7	27.7	35.1	
3				7	9	4	6	6	0	2	3	7	6	5	8	0	7		
	(5.88)	(6.09	(12.2	(7.90	(13.7	(27.1	(28.3	(30.6	(35.1	(22.	(23.	(26.	(21.	(23.	(28.	(23.	(27.	(34.	
)	4))	0)	7)	7)	4)	0)	93)	45)	66)	51)	61)	17)	10)	30)	70)		
2	2.52	2.61	4.06	3.04	4.40	9.59		11.1	15.0	15.7	7.53	8.68	9.31	6.95	8.02	9.08	7.53	8.80	10.5
							1	8	7									9	
	(2.48)	(2.58	(4.09	(3.03	(4.44	(8.76	(9.76	(11.2	(11.5	(8.3	(8.5	(8.4	(7.3	(7.8	(8.4	(7.3	(8.1	(9.7	
)))))))	4)	1)	7)	2)	4)	3)	0)	1)	3)	6)	7)	
4	1.60	1.63	2.07	1.77	2.14	3.16	3.42	4.13	4.33	2.40	2.70	2.93	2.30	2.57	2.82	2.52	2.77	3.10	
	(1.19)	(1.21	(1.61	(1.35	(1.67	(2.45	(2.64	(3.13	(3.21	(2.3	(2.5	(2.6	(2.0	(2.2	(2.3	(2.0	(2.2	(2.4	
)))))))))	6)	8)	1)	6)	5)	6)	4)	3)	9)	
<i>EQL</i>	17.35	17.8	28.3	20.9	30.5	58.9	65.6	81.0	84.5	45.0	50.8	55.8	43.2	49.2	55.8	47.5	54.5	63.8	
<i>RARL</i>	1.00	1.00	1.00	1.21	1.71	2.08	3.78	4.53	2.99	2.59	2.85	1.97	2.49	2.76	1.97	2.74	3.05	2.25	
<i>PCI</i>	1.00	1.00	1.00	1.24	1.84	2.28	4.82	5.86	3.47	3.17	3.47	2.15	3.02	3.34	2.14	3.35	3.75	2.49	

Table 2. ARL and SDRL values for the two-sided THWMA TBE chart and two-sided competing charts when $k = 1$ and $ARL_0 \cong 370$.

		THWMA TBE			DHWMA TBE			HWMA TBE			TEWMA TBE			DEWMA TBE			EWMA TBE										
		$\varphi = 0.05$		0.1	0.2	0.05		0.1	0.2	0.05		0.1	0.2	0.05		0.1	0.2	0.05		0.1	0.2	0.05		0.1	0.2		
δ	$L =$	1.245		1.57		1.342		1.65		2.99		4.021		1.72		2.02		2.34		1.92		2.21		2.566		2.53	
		1.196	8	9		8	2.65	8		8	2.99	4.021		4	2	2	64	3	64	2.566	6	2.53	2.936				
0.2	5	4.06	4.27	5.91		4.75	6.35	13.3		16.5		33.21		8.51	10.5	11.7		8.39	10.1	13.23		12.2		20.68			
		(1.10)	(1.15)	(1.4)		(1.19)	(1.4)	(2.2)		(2.6)		(4.70)		(2.4)	(2.2)	(2.1)		(2.0)	(2.0)	(3.19)		(2.3)		(5.27))		
0.5	0.5	6.90	7.38	11.1		8.41	12.1	28.1		35.9		104.2		18.4	21.2	28.2		17.9	21.8	50.10		27.6		130.3			
		(4.11)	(4.34)	(5.7)		(4.76)	(6.1)	(9.9)		(11.)		(36.5)		(9.0)	(8.6)	(15.)		(8.1)	(9.5)	(36.4)		(11.)		(105.))		
0.7	0.7	12.93	14.18	24.7		16.93	27.6	72.1		97.8		34813		42.7	52.5	115.		43.5	62.5	357.8		85.6		2715.			
		(13.1)	(14.1)	(20.)		(16.1)	(22.)	(38.)		(48.)		(2782)		(28.)	(36.)	(101)		(28.)	(47.)	(344.)		(62.)		(269))		
0.8	0.8	20.07	22.76	45.7		28.94	51.7	156.		241.		5637.		78.9	110.	299.		85.5	141.	1010.		218.		5322.			
		(28.0)	(31.0)	(48.)		(36.7)	(52.)	(104)		(160)		(5150)		(63.)	(95.)	(292)		(71.)	(128)	(101)		(197)		(536))		
0.8	0.8	27.14	31.65	69.5		41.40	80.0	275.		507.		2301.		120.	174.	465.		133.	229.	1239.		373.		2780.			
		(45.7)	(51.3)	(85.)		(62.3)	(92.)	(206)		(397)		(2073)		(109)	(163)	(466)		(123)	(221)	(125)		(363)		(283))		
0.9	0.9	40.01	48.88	123.		67.82	143.	520.		939.		1078.		196.	279.	596.		220.	357.	995.9		570.		1304.			
		(86.2)	(100.)	(177)		(126.)	(192)	(405)		(768)		(893.)		(197)	(279)	(608)		(221)	(362)	(101)		(583)		(133))		
0.9	0.9	52.68	65.78	178.		95.64	207.	606.		842.		796.0		255.	341.	593.		282.	414.	795.4		610.		917.4			
		(135.)	(161.)	(279)		(204.)	(296)	(464)		(652)		(613.)		(268)	(349)	(607)		(295)	(425)	(818.)		(637)		(941.))		
0.9	0.9	75.65	98.83	271.		148.5	304.	576.		645.		602.4		317.	390.	533.		342.	440.	620.2		562.		658.2			
		(247.)	(293.)	(451)		(376.)	(448)	(436)		(483)		(474.)		(345)	(405)	(548)		(365)	(455)	(638.)		(587)		(678.))		
0.9	0.9	137.7	186.9	373.		276.9	385.	469.		485.		470.0		366.	400.	453.		378.	422.	475.6		471.		487.4			
		(660.)	(787.)	(620)		(865.)	(562)	(355)		(351)		(329.)		(407)	(420)	(468)		(412)	(445)	(492.)		(498)		(504.))		
0.9	0.9	5	3	03		5	61	00		22		7		96	83	56		57	42	8		63		4			
		(63.)	(71.)	(.58)		(85.)	(.59)	(.24)		(.94)		(00)		(.57)	(.35)	(.97)		(.32)	(.72)	(.88)		(.19)		(.08))		

Continued no next page

	370.8	370.3	370.	370.1	370.	369.	371.	369.8	370.	369.	370.	370.	369.	369.6	370.	370.7	
1	3	7	66	6	81	47	57	0	47	57	74	12	80	2	56	2	
	(3407)	(210)	(608)	(120)	(538)	(277)	(267)	(273)	(417)	(392)	(383)	(408)	(391)	(381)	(395)	(384)	
	.25)	1.21)	.74)	1.00)	.00)	.37)	.51)	54)	.93)	.42)	.12)	.78)	.29)	.49)	.69)	16)	
1.0	135.9	176.8	279.	229.5	289.	285.	291.	299.2	325.	315.	296.	323.	308.	291.8	285.	283.3	
25	5	1	98	3	88	36	52	3	67	84	33	47	79	8	86	3	
	(676.	(711.	(454	(659.	(416	(216	(206	(218.	(366	(337	(307	(356	(325	(301.	(305	(294.	
	18)	54)	.23)	57)	.51)	.02)	.80)	42)	.08)	.43)	.98)	.64)	.72)	30)	.63)	46)	
1.0	75.25	96.58	197.	138.7	209.	227.	234.	247.7	262.	256.	238.	257.	247.	231.8	221.	224.0	
5			17	0	81	21	86	2	45	72	15	89	21	1	02	9	
	(265.	(306.	(313	(344.	(296	(172	(165	(176.	(294	(272	(248	(285	(261	(241.	(236	(232.	
	52)	37)	.87)	39)	.39)	.50)	.36)	95)	.58)	.91)	.81)	.97)	.29)	36)	.76)	60)	
1.0	48.68	60.39	133.	85.09	145.	176.	185.	200.3	197.	196.	185.	195.	189.	179.1	163.	173.1	
8			83		83	82	21	1	61	84	07	15	95	6	65	0	
	(134.	(156.	(205	(189.	(200	(135	(131	(139.	(218	(208	(192	(213	(201	(186.	(175	(178.	
	61)	90)	.13)	95)	.82)	.09)	.37)	15)	.49)	.43)	.20)	.58)	.33)	42)	.17)	67)	
1.1	36.03	43.49	96.0	59.63	104.	140.	150.	166.6	149.	151.	145.	147.	146.	141.3	126.	134.9	
1			1		04	75	17	8	32	72	06	91	49	1	18	6	
	(84.1	(97.3	(143	(121.	(142	(108	(107	(114.	(161	(159	(149	(160	(154	(146.	(134	(140.	
	7)	7)	.66)	32)	.78)	.83)	.57)	83)	.63)	.10)	.35)	.91)	.09)	63)	.52)	03)	
1.1	22.43	26.23	52.0	32.96	56.7	90.2	98.1	114.0	85.9	89.7	89.7	84.1	86.5	88.39	74.6	85.02	
8			4		2	0	9	3	9	0	7	6	6		8		
	(42.0	(48.0	(74.	(56.8	(75.	(72.	(71.	(76.8	(89.	(91.	(92.	(88.	(90.	(91.3	(78.	(87.1	
	0)	6)	25)	1)	62)	04)	68)	9)	04)	46)	18)	80)	12)	8)	78)	8)	
1.2	16.54	18.28	32.9	22.31	36.3	62.7	69.4	83.22	57.3	59.2	60.3	54.7	57.2	60.11	50.1	57.39	
5			5		5	6	5		8	3	6	2	8		9		
	(26.7	(29.1	(44.	(34.3	(47.	(51.	(52.	(55.8	(56.	(58.	(60.	(56.	(58.	(61.3	(52.	(58.5	
	6)	9)	90)	6)	66)	93)	22)	0)	95)	64)	70)	43)	20)	3)	02)	7)	
1.4	9.66	10.36	15.7	11.98	17.1	31.1	35.5	45.23	28.5	29.0	29.1	26.0	27.1	28.80	23.9	27.85	
3			4		2	7	8		1	3	5	4	3		8		
	(12.6	(13.4	(19.	(15.4	(20.	(27.	(28.	(30.6	(27.	(27.	(27.	(25.	(26.	(28.6	(24.	(27.4	
	4)	3)	39)	0)	73)	61)	64)	4)	70)	12)	94)	85)	50)	3)	35)	8)	
2	4.59	4.78	5.87		5.10	6.16	9.71	11.2	15.05	9.55	9.85	9.70	8.38	8.80	9.12	7.78	8.88
								0									
	(4.50)	(4.73	(5.8	(5.02	(6.1	(8.9	(9.7	(11.2	(9.8	(9.3	(8.7	(8.4	(8.3	(8.45	(7.5	(8.25	
)	2))	1)	1)		5)	3)	4)	2)	2)	4)	4))	1))	
4	2.26	2.29	2.51		2.36	2.56	3.19		3.43	4.12		2.77	2.96	3.01	2.56	2.71	2.84
															2.58	2.80	
	(1.75)	(1.79	(1.9	(1.85	(2.0	(2.4		(2.6		(2.7	(2.8	(2.6	(2.3	(2.3	(2.40	(2.0	(2.25
)	6))	1)	7)		4)		6)	4)	8)	1)	7))	9))	
<i>EQL</i>	27.27	29.39		41.8		44.3	69.8	83.8	864.1	57.7	62.1	73.4	55.2	61.4	98.33	63.9	218.1
						33.48		0	1	9	2	2	3	9	1	0	
<i>RARI</i>	1.00	1.00	1.00		1.23	1.51	1.67	3.08	29.41	2.12	2.11	1.76	2.02	2.09	2.35	2.35	7.42
<i>PCI</i>	1.00	1.00	1.00		1.19	1.49	1.80	3.62		107.9		2.29	2.32	1.94	2.16	2.30	2.90
									4			1)	7))	9))	

Table 3. ARL and SDRL values for the one-sided THWMA TBE chart and one-sided competing charts when $k = 2$ and $ARL_0 \cong 370$.

THWMA TBE				DHWMA TBE			HWMA TBE			TEWMA TBE			DEWMA TBE			EWMA TBE			
$\varphi =$	0.05	0.1	0.2	0.05	0.1	0.2	0.05	0.1	0.2	0.05	0.1	0.2	0.05	0.1	0.2	0.05	0.1	0.2	
δ	0.264 8	0.24	0.42	0.26	0.48	0.92	0.99	1.18	1.29	1.27	1.58	1.85	1.48	1.77	1.97	1.95	2.05	2.01	
		86	5		2	3	6	2	2	4	67	1	4	2	9	6		9	
		370.0	370.		370.	369.	371.	371.	369.	369.	370.	370.	370.	370.	369.	370.	370.	370.	
1	4	62	59	50	81	16	47	90	42	56	73	06	85	56	36	92	90	50	
	(3663.	(366	(263	(352	(235	(117	(109	(976	(926	(424	(382	(367	(405	(376	(367	(375	(368	(364	
	81)	4.86)	4.21)	2.26)	2.97)	2.64)	9.43)	.50)	.19)	.16)	.36)	.65)	.37)	.01)	.81)	.94)	.62)	.07)	
0.9	34.92	33.9	51.4	35.1	58.0	108.	115.	124.	128.	225.	247.	267.	231.	253.	275.	250.	269.	288.	
		6	0	2	3	62	61	45	47	65	29	39	12	49	64	28	24	14	
		(191.9	(185.	(217.	(183.	(227.	(248.	(248.	(240	(247	(253	(251	(264	(249	(253	(271	(250	(264	(283
0.9	15.53	2)	23)	46)	92)	55)	28)	15)	.14)	.24)	.76)	.08)	.01)	.66)	.53)	.10)	.63)	.29)	.75)
		15.3	23.3	15.6	26.5	57.2	61.6	69.2	71.0	148.	171.	197.	153.	178.	206.	174.	197.	226.	
		8	6	3	2	4	6	1	4	05	65	61	53	04	07	35	99	38	
0.9	10.09	(61.76	(61.5	(77.6	(60.7	(83.0	(111.	(112.	(111	(114	(162	(170	(193	(162	(175	(201	(169	(192	(221
)	9)	6)	6)	0)	45)	40)	.90)	.95)	.06)	.39)	.62)	.03)	.61)	.72)	.99)	.49)	.20)
		9.81	14.6	10.2	16.6	36.3	39.7	45.5	46.6	101.	121.	145.	106.	128.	157.	124.	147.	177.	
0.9	25	1	4	7	2	2	2	2	3	69	52	96	61	34	04	97	54	85	
		(32.21	(31.3	(41.3	(33.2	(45.1	(64.4	(65.7	(65.	(66.	(106	(117	(139	(109	(124	(152	(119	(141	(172
)	7)	6)	1)	3)	2)	1)	51)	88)	.81)	.40)	.90)	.26)	.14)	.35)	.93)	.71)	.87)
0.9	7.27	10.3	7.29	11.5	25.6	28.2	33.1	34.0	73.4	90.1	111.	77.4	95.8	120.	92.8	113.	141.	141.	
		3	2	6	1	8	9	1	1	64	7	4	81	4	54	06			
		(19.26	(20.1	(25.8	(19.5	(27.8	(41.8	(43.0	(43.	(44.	(74.	(84.	(104	(76.	(89.	(115	(86.	(106	(135
0.8	4.67)	1)	0)	2)	0)	8)	9)	80)	45)	90)	31)	.72)	77)	60)	.22)	07)	.79)	.89)
		4.61	6.38	4.71	7.01	5	1	7	3	7	5	8	3	9	1	9	3	0	
		(9.40	(12.8	(9.67	(13.6	(21.9	(22.9	(23.	(23.	(41.	(46.	(60.	(42.	(49.	(67.	(47.	(60.	(84.	
0.8	3.53)	1))	6)	5)	0)	46)	34)	95)	27)	26)	03)	60)	88)	22)	89)	32)	
		3.46	4.50	3.54	4.96	10.2	11.4	13.9	14.6	29.1	35.6	43.7	29.6	36.8	47.5	36.5	44.8	59.3	
		(5.79	(7.58	(5.99	(8.11	(13.2	(13.8	(14.	(14.	(26.	(27.	(36.	(25.	(29.	(40.	(28.	(36.	(53.	
0.8	(5.83)))))	3)	5)	48)	58)	69)	82)	24)	42)	66)	97)	44)	83)	23)	
		2.33	2.32	2.85	2.33	3.09	5.84	6.47	8.11	8.53	15.2	19.0	21.9	15.4	19.0	23.1	19.1	22.4	28.5
		(2.84)	(2.80	(3.42	(2.80	(3.77	(6.12	(6.43	(6.9	(6.8	(13.	(12.	(14.	(11.	(12.	(16.	(12.	(15.	(22.
0.5	1.42	1.61	1.42	1.71	2.85	3.12	3.90	4.15	5.73	7.88	8.98	6.06	7.81	8.85	8.06	8.99	9.88		
		(1.05)	(1.04	(1.27	(1.05	(1.35	(2.04	(2.12	(2.2	(2.1	(4.2	(4.2	(3.9	(3.6	(3.8	(4.0	(3.6	(4.0	(5.1
)))))))	5)	9)	4)	9)	7)	2))	2))	8)	

Continued on next page

0.2																		
5	1.02	1.02	1.05	1.02	1.06	1.45	1.59	2.10	2.32	2.29	3.47	4.33	2.73	3.67	4.23	3.94	4.31	4.35
	(0.22)	(0.21)	(0.31)	(0.21)	(0.36)	(0.85)	(0.92)	(0.9)	(0.8)	(1.0)	(1.1)	(1.1)	(0.8)	(0.9)	(0.9)	(0.9)	(0.9)	(1.0)
)))))))	8)	0)	5)	5))	8)	6)	8)	1)	8)	7)
<i>EQL</i>	9.13	9.08	10.3	9.14	10.8	15.6	16.4	17.8	18.1	29.5	33.6	38.1	30.3	34.6	40.0	34.2	38.5	44.6
			5		4	1	1	1	9	8	7	8	9	8	4	2	7	2
<i>RARL</i>	1.00	1.00	1.00	1.00	1.19	1.51	1.80	1.96	1.76	3.24	3.71	3.69	3.33	3.82	3.87	3.75	4.25	4.31
<i>PCI</i>	1.00	1.00	1.00	1.00	1.32	1.93	2.61	3.24	2.76	5.71	7.36	6.92	5.97	7.53	7.21	7.47	8.83	8.41
$\varphi =$																		
0.05	0.1	0.2	0.05	0.1	0.2	0.05	0.1	0.2	0.05	0.1	0.2	0.05	0.1	0.2	0.05	0.1	0.2	
δ	<i>L</i> =	0.12	0.81	0.34	0.95	2.33	2.65	3.56	4.07	1.31	1.73	2.19	1.56	1.99	2.46	2.38	2.79	3.24
	0.113	7	7	8	5	7	4	2	1	1	5	7	8	1	2	5	1	3
1	370.3	370.	370.	370.	370.	370.	370.	371.	370.	370.	370.	370.	369.	370.	370.	370.	370.	370.
	9	03	46	38	84	47	19	04	94	10	18	40	38	46	20	32	55	80
	(3697.	(318	(823.	(176	(709.	(305.	(284.	(283	(326	(436	(404	(385	(426	(398	(381	(398	(383	(374
	96)	5.63)	02)	0.16)	15)	28)	30)	.56)	.31)	.65)	.40)	.94)	.39)	.10)	.75)	.74)	.75)	.87)
1.0	38.2	132.	63.9	150.	244.	253.	270.	281.	219.	238.	256.	225.	243.	262.	241.	259.	277.	
25	37.41	2	72	5	61	94	96	61	92	62	99	05	87	72	16	04	09	07
	(181.1	(181.	(287.	(237.	(285.	(202.	(192.	(198	(241	(257	(259	(267	(260	(261	(270	(260	(268	(280
	1)	49)	58)	88)	14)	57)	20)	.59)	.43)	.38)	.87)	.41)	.51)	.62)	.74)	.66)	.48)	.80)
1.0	19.4	69.4	31.3	82.6	173.	184.	206.	221.	144.	163.	184.	148.	169.	191.	166.	189.	213.	
5	18.15	4	7	5	7	99	46	26	36	32	18	02	84	62	89	62	32	05
	(65.30	(71.3	(143.	(96.7	(152.	(144.	(139.	(147	(186	(166	(176	(191	(170	(181	(198	(179	(195	(216
)	4)	30)	4)	44)	69)	11)	.63)	.08)	.34)	.73)	.53)	.51)	.60)	.47)	.07)	.84)	.13)
1.0	12.0	40.1	18.2	48.0	122.	134.	155.	169.	95.7	111.	131.	98.4	116.	136.	114.	134.	158.	
8	11.53	3	9	9	4	88	15	75	31	0	20	07	9	29	98	33	82	32
	(32.04	(33.6	(78.9	(47.3	(85.5	(103.	(102.	(109	(139	(108	(118	(135	(111	(123	(141	(122	(138	(160
)	9)	5)	9)	7)	25)	14)	.04)	.11)	.51)	.62)	.34)	.18)	.57)	.47)	.12)	.84)	.80)
1.1	26.6	12.8	32.3	90.9	100.	121.	133.	68.8	80.9	95.8	70.1	84.3	101.	81.5	99.3	121.		
1	8.67	8.76	9	7	9	5	71	08	53	2	7	7	4	4	61	8	3	84
	(20.45	(20.5	(49.7	(28.7	(56.2	(77.7	(77.4	(83.	(108	(76.	(84.	(98.	(77.	(88.	(104	(86.	(101	(123
)	9)	7)	3)	2)	7)	9)	53)	.24)	54)	43)	45)	86)	95)	.06)	27)	.85)	.23)
1.1	14.2	7.83	16.8	51.9	59.4	74.9	82.4	38.7	44.9	53.7	38.1	46.3	56.9	44.6	55.4	70.8		
8	5.71	5.81	8	3	9	5	5	7	0	9	3	9	9	2	4	7	1	8
	(10.42	(10.6	(23.2	(13.9	(26.1	(45.7	(46.8	(50.	(63.	(41.	(45.	(53.	(41.	(47.	(57.	(45.	(55.	(70.
)	8)	7)	3)	9)	9)	8)	81)	90)	86)	00)	40)	15)	44)	26)	76)	29)	57)
1.2	11.1	4.44	9.65	5.68	11.1	33.6	39.3	51.3	56.2	25.6	29.4	34.5	24.9	29.9	36.3	28.6	35.5	45.6
5				4	0	8	0	6	2	2	9	4	9	3	8	0	6	
	(6.74)	(6.85	(14.0	(8.84	(15.7	(30.3	(32.0	(34.	(41.	(27.	(28.	(33.	(26.	(29.	(36.	(28.	(34.	(44.
)	6))	3)	1)	0)	68)	96)	29)	53)	41)	31)	77)	05)	48)	67)	95)	
1.4	2.96	3.03	5.35	3.63	5.94	15.4	18.4	25.3	27.4	12.6	14.5	16.2	11.8	13.9	16.4	13.3	16.1	20.2
3				9	0	8	1	2	7	4	8	9	3	1	1	2		

Continued on next page

	(3.41)	(3.55)	(6.29)	(4.30)	(6.87)	(14.3)	(15.6)	(17.)	(19.)	(13.)	(13.)	(14.)	(12.)	(13.)	(15.)	(12.)	(14.)	(19.)
)))))	1)	1)	62)	58)	76)	82)	68)	42)	36)	23)	75)	97)	07)
2	1.85	1.87	2.62	2.08	2.81	5.11	5.78	7.84	8.53	4.11	4.90	5.39	3.91	4.57	5.17	4.40	5.10	5.94
	(1.56)	(1.57)	(2.29)	(1.78)	(2.43)	(4.26)	(4.69)	(5.7)	(6.0)	(4.4)	(4.8)	(4.7)	(3.9)	(4.2)	(4.4)	(3.8)	(4.3)	(5.0)
)))))))	9)	2)	9)	0)	4)	0)	6)	7)	8)	5)	0)
4	1.22	1.23	1.42	1.29	1.47	1.97	2.08	2.41	2.48	1.48	1.61	1.76	1.48	1.61	1.74	1.64	1.76	1.91
	(0.69)	(0.70)	(0.93)	(0.77)	(0.98)	(1.37)	(1.45)	(1.6)	(1.6)	(1.0)	(1.2)	(1.3)	(0.9)	(1.0)	(1.1)	(1.0)	(1.1)	(1.2)
)))))))	3)	6)	7)	0)	2)	6)	8)	9)	3)	4)	6)
<i>EQL</i>	13.27	13.4	18.9	14.8	20.3	35.8	39.4	48.8	52.1	28.5	32.3	35.9	28.1	31.9	36.0	31.3	35.6	41.2
	1	5	9	7	5	6	5	6	4	3	1	0	3	1	5	9	8	
<i>RARL</i>	1.00	1.00	1.00	1.12	1.52	1.89	2.97	3.64	2.75	2.15	2.41	1.90	2.12	2.38	1.90	2.36	2.66	2.18
<i>PCI</i>	1.00	1.00	1.00	1.15	1.64	2.02	3.77	4.80	3.17	2.63	3.00	2.05	2.56	2.92	2.03	2.88	3.32	2.37

Table 4. ARL and SDRL values for the two-sided THWMA TBE chart and two-sided competing charts when $k = 2$ and $ARL_0 \cong 370$.

		THWMA TBE			DHWMA TBE			HWMA TBE			TEWMA TBE			DEWMA TBE			EWMA TBE				
		$\varphi =$	0.1	0.2		0.05	0.1	0.2		0.05	0.1	0.2		0.05	0.1	0.2		0.05	0.1		
δ	$L =$	1.248	1.57		1.342	1.64	2.48		2.72	3.56		1.73	2.02	2.34		1.93	2.22	2.54		2.52	2.81
		1.2124	3	1		1	4		9	65	4	7		8	6	04		6	1		
0.2 5	2.50	2.67	3.68		3.13	3.87	6.65		7.63	11.83		4.32	5.57	6.58		4.42	5.50	6.55		6.26	7.90
	(1.09)	(1.04)	(0.7)		(0.77)	(0.8)	(1.0)		(1.1)	(1.63)		(1.3)	(1.3)	(1.2)		(1.1)	(1.1)	(1.1)		(1.1)	(1.4)
0.5	4.36	4.57	6.40		5.14	6.85	13.2		15.6	26.97		10.0	11.9	13.4		9.72	11.6	14.8		13.3	19.2
	(2.39)	(2.41)	(2.9)		(2.49)	(3.0)	(4.6)		(5.1)	(7.92)		(5.2)	(4.9)	(5.1)		(4.5)	(4.5)	(6.7)		(4.9)	(8.2)
0.7	8.12	8.66	13.7		10.07	14.9	32.8		39.3	91.36		24.7	28.2	39.7		24.2	29.8	57.9		35.1	83.1
	(7.24)	(7.60)	(10.)		(8.46)	(11.)	(17.)		(19.)	(46.0)		(16.)	(16.)	(28.)		(15.)	(18.)	(47.)		(20.)	(67.)
0.8	13.00	14.06	25.4		17.08	28.1	66.9		82.2	508.5		46.6	56.5	101.		47.6	65.6	170.		78.8	301.
	(15.82)	(16.8)	(25.)		(19.4)	(26.)	(42.)		(49.)	(482.)		(34.)	(43.)	(90.)		(35.)	(53.)	(161.)		(61.)	(285.)
0.8 5	17.75	19.47	39.0		24.61	43.8	110.		141.	6831.		71.5	92.3	180.		75.7	112.	316.		138.	622.
	(26.12)	(28.2)	(45.)		(33.6)	(48.)	(78.)		(97.)	(765)		(59.)	(80.)	(172)		(64.)	(101)	(311)		(122)	(616)
)	9)	00)		3)	05)	50)		22)	7.19)		84)	10)	.74)		72)	.91)	.37)		.64)	.53)

Continued on next page

0.9	27.27	30.90	70.2	40.68	79.5	223.	312.	2177.	126.	168.	325.	138.	209.	522.	270.	965.	
			3		9	35	16	35	06	48	05	11	80	35	19	20	
	(52.06	(56.8	(94.	(69.1	(101	(181	(247	(195	(120	(162	(325	(133	(206	(526	(262	(972	
))	3)	87)	3)	.44)	.21)	.86)	6.29)	.42)	.20)	.12)	.67)	.71)	.26)	.08)	.64)	
0.9	35.79	41.15	103.	57.66	119.	340.	493.	1267.	178.	234.	406.	195.	283.	585.	368.	907.	
25			28		41	92	19	32	63	27	70	39	77	75	11	37	
	(80.41	(88.3	(155	(111.	(167	(281	(400	(108	(183	(234	(410	(199	(287	(596	(369	(929	
))	1)	.41)	15)	.01)	.08)	.90)	8.34)	.11)	.79)	.70)	.30)	.50)	.06)	.47)	.04)	
0.9	53.01	63.09	173.	91.50	200.	470.	616.	795.2	256.	312.	457.	276.	363.	563.	451.	713.	
5			19		33	61	33	2	90	35	21	29	28	63	17	63	
	(148.0	(168.	(291	(213.	(307	(378	(494	(650.	(277	(323	(468	(292	(374	(573	(464	(733	
1)	14)	.41)	71)	.89)	.40)	.36)	93)	.77)	.19)	.12)	.48)	.80)	.44)	.18)	.5)		
0.9	96.63	122.9	314.	188.9	336.	478.	524.	526.9	340.	370.	440.	358.	396.	479.	450.	517.	
75		0	54	1	54	31	34	9	49	12	21	29	09	74	31	20	
	(399.2	(462.	(566	(576.	(533	(381	(407	(414.	(379	(388	(452	(391	(416	(494	(470	(532	
5)	24)	.50)	53)	.77)	.25)	.85)	94)	.45)	.14)	.75)	.77)	.19)	.20)	.18)	.42)		
1	370.76	370.1	370.	370.2	369.	370.	370.	370.7	370.	360.	370.	370.	369.	370.	369.	370.	
	0	72	2	36	55	77	1	49	45	99	24	78	52	92	02		
	(3429.	(231	(656	(131	(576	(295	(283	(281.	(421	(384	(384	(412	(387	(378	(392	(379	
71)	6.02)	.82)	2.93)	.58)	.23)	.80)	38)	.77)	.40)	.66)	.63)	.83)	.78)	.20)	.46)		
1.0	100.37	119.8	241.	170.4	250.	264.	263.	271.3	306.	294.	288.	303.	294.	279.	270.	264.	
25		6	15	3	30	85	26	8	46	53	77	65	27	45	12	97	
	(433.3	(449.	(415	(498.	(382	(212	(197	(199.	(348	(313	(299	(339	(310	(287	(285	(273	
3)	81)	.76)	46)	.51)	.00)	.20)	44)	.41)	.34)	.96)	.29)	.99)	.76)	.41)	.68)		
1.0	53.19	62.92	144.	89.49	157.	191.	194.	205.7	219.	220.	217.	220.	220.	210.	195.	191.	
5			12		51	07	87	2	98	83	12	22	20	24	12	84	
	(160.0	(179.	(235	(214.	(232	(152	(145	(148.	(246	(234	(223	(241	(231	(216	(207	(198	
1)	06)	.31)	58)	.71)	.90)	.33)	19)	.69)	.13)	.60)	.41)	.86)	.63)	.13)	.87)		
1.0	33.19	38.99	87.5	53.04	96.6	136.	140.	155.5	146.	153.	156.	148.	152.	150.	133.	137.	
8		8	33	0	33	32	1	29	25	75	22	45	59	85	92		
	(78.37	(90.7	(136	(110.	(138	(109	(104	(109.	(157	(159	(161	(159	(159	(154	(140	(141	
)	8)	.27)	29)	.38)	.93)	.92)	02)	.93)	.64)	.23)	.64)	.70)	.14)	.61)	.88)		
1.1	24.47	27.73	58.5	36.62	65.0	101.	106.	120.8	103.	109.	114.	102.	110.	111.	95.7	101.	
1			4		7	11	67	5	06	20	67	39	08	39	5	44	
	(50.32	(55.4	(87.	(67.9	(89.	(82.	(80.	(83.6	(107	(111	(116	(108	(113	(113	(99.	(103	
)	7)	33)	9)	77)	38)	57)	2)	.50)	.29)	.86)	.03)	.75)	.81)	36)	.30)		
1.1	15.08	16.47	29.9	19.98	32.7	57.8	62.3	74.77	55.1	58.4	62.4	53.2	57.8	61.8	51.4	56.7	
8			4		9	1	1		2	4	4	9	3	5	8	6	
	(24.64	(26.6	(40.	(30.8	(42.	(48.	(48.	(50.5	(54.	(56.	(61.	(53.	(57.	(62.	(51.	(56.	
)	5)	88)	5)	73)	64)	29)	8)	05)	98)	98)	88)	80)	19)	79)	68)		
1.2	10.74	11.52	18.9	13.61	20.7	37.4	41.1	51.57	35.5	37.0	39.2	33.3	36.1	39.1	32.1	36.1	
5			5		3	0	5		1	2	3	3	3	9	5	2	

Continued on next page

	(15.11)	(16.0)	(24.)	(18.6)	(25.)	(32.)	(32.)	(34.7)	(34.)	(34.)	(37.)	(32.)	(34.)	(38.)	(31.)	(35.)	
)	7)	28)	5)	65)	44)	86)	5)	02)	47)	66)	86)	95)	80)	67)	29)		
1.4	6.31	6.63	9.28	7.36	9.85	16.9	19.1	25.31	17.0	17.4	17.8	15.2	16.2	17.4	14.7	16.2	
3						9	7		0	6	6	9	5	0	2	9	
	(7.11)	(7.51)	(10.)	(8.19)	(10.)	(15.)	(16.)	(17.6)	(16.)	(15.)	(15.)	(14.)	(14.)	(16.)	(13.)	(15.)	
))	18))	64)	30)	08)	5)	50)	59)	93)	78)	94)	15)	84)	13)		
2	3.07	3.15	3.72	3.32	3.83	5.47	5.97	7.81	5.26	5.63	5.78	4.73	5.12	5.35	4.68	5.13	
	(2.62)	(2.69)	(3.1)	(2.83)	(3.2)	(4.4)	(4.8)	(5.79)	(5.4)	(5.3)	(4.9)	(4.5)	(4.6)	(4.5)	(4.1)	(4.3)	
))	7))	6)	9)	1))	1)	1)	9)	9)	6)	8)	0)	7)		
4	1.56	1.58	1.69	1.61	1.72	2.02	2.11	2.41	1.65	1.74	1.82	1.61	1.70	1.77	1.68	1.77	
	(1.08)	(1.09)	(1.1)	(1.12)	(1.2)	(1.4)	(1.4)	(1.64)	(1.2)	(1.3)	(1.3)	(1.1)	(1.1)	(1.2)	(1.0)	(1.1)	
))	9))	0)	2)	8))	9)	6)	7)	2)	8)	1)	7)	4)		
<i>EQL</i>	19.35	20.33		28.3		29.8	44.2	49.6	147.7	38.1	40.9	47.1	37.1	41.2	52.0	41.4	62.4
				4		5	4	3	9	4	2	2	8	2	6	7	5
<i>RARI</i>	1.00	1.00	1.00	1.18	1.47	1.56	2.57	7.27	1.97	2.01	1.66	1.92	2.03	1.84	2.14	3.07	
<i>PCI</i>	1.00	1.00	1.00	1.15	1.40	1.62	2.74	9.36	2.04	2.12	1.73	1.95	2.10	1.89	2.26	3.54	

Table 5. ARL and SDRL values for the one-sided THWMA TBE chart and one-sided competing charts when $k = 3$ and $ARL_0 \cong 370$.

THWMA TBE			DHWMA TBE			HWMA TBE			TEWMA TBE			DEWMA TBE			EWMA TBE			
$\varphi =$	0.05	0.1	0.2	0.05	0.1	0.2	0.05	0.1	0.2	0.05	0.1	0.2	0.05	0.1	0.2	0.05	0.1	0.2
$L =$																		
δ	0.255	0.23	0.45	0.24	0.52	1.02	1.11	1.35	1.49	1.28	1.60	1.88	1.49	1.79	2.02	1.99	2.11	2.11
	5	9	3	8	7	7	5	8	8	3	5	7	4	7	3	27	7	
1	370.9	370.	370.	370.	370.	369.	371.	370.	371.	370.	370.	370.	369.	370.	370.	370.	370.	
	6	12	93	00	21	95	01	58	55	49	14	34	90	19	72	20	24	94
	(3721.	(361	(234	(345	(199	(939	(873	(754	(689	(426	(382	(368	(408	(378	(370	(378	(368	(365
	91)	6.66	3.56)	9.97)	0.35)	.73)	.45)	.19)	.41)	.80)	.08)	.26)	.86)	.92)	.67)	.58)	.98)	.70)
0.9	27.1	45.7	27.8	52.8	106	113.	128.	138.	204.	226.	248.	210.	232.	256.	227.	249.	272.	
75	27.72	5	3	3	8	60	82	03	54	44	41	95	03	40	98	90	00	92
	(145.8	(129.	(172.	(129.	(183.	(208	(206	(203	(215	(232	(231	(246	(229	(234	(253	(228	(245	(270
	1)	84)	09)	13)	32)	.08)	.49)	.65)	.66)	.50)	.09)	.62)	.07)	.24)	.69)	.96)	.46)	.16)
0.9	12.6	20.6	12.9	23.6	54.2	59.7	69.9	75.5	123.	146.	172.	129.	152.	180.	148.	172.	201.	
5	12.93	1	6	5	6	0	0	7	6	74	16	62	79	74	87	32	27	74
	(45.52	(44.4	(61.2	(44.8	(65.9	(92.	(94.	(96.	(103	(135	(145	(167	(136	(151	(177	(145	(167	(198
)	5)	6)	5)	4)	63)	27)	04)	.22)	.79)	.26)	.87)	.95)	.23)	.17)	.84)	.28)	.39)
0.9	8.20	8.02	12.5	8.22	14.5	34.3	38.0	45.3	49.2	81.7	99.2	121.	85.1	103.	130.	100.	122.	151.
25		8)		1	8	0	0	3	6	5	9	39	5	85	07	81	41	09
	(22.85	(22.8	(32.0	(23.0	(34.9	(53.	(55.	(56.	(61.	(86.	(95.	(116	(86.	(99.	(125	(95.	(116	(146
)	2)	3)	8)	8)	66)	06)	30)	05)	69)	49)	.42)	89)	74)	.19)	42)	.93)	.05)

Continued on next page

0.9	6.01	5.98	8.92	6.04	10.0	23.6	26.5	32.7	35.1	57.4	70.3	88.4	59.7	74.5	96.2	72.6	89.2	114.	
	(14.06)	(14.2)	(19.7)	(14.2)	(21.3)	(34.)	(36.)	(37.)	(39.)	(58.)	(65.)	(82.)	(58.)	(69.)	(90.)	(66.)	(82.)	(109.)	
)	1)	2)	7)	5)	37)	01)	37)	38)	34)	11)	13)	24)	34)	90)	34)	90)	.56)	
0.8	3.91	3.94	5.50	3.96	6.11	13.8	15.6	19.4	20.9	33.1	40.6	50.2	33.8	42.4	55.0	41.4	51.4	68.3	
5	(7.03)	(7.00)	(9.72)	(7.12)	(10.5)	(17.)	(18.)	(19.)	(20.)	(31.)	(33.)	(43.)	(30.)	(36.)	(49.)	(34.)	(44.)	(63.)	
))))	7)	85)	77)	60)	49)	76)	80)	39)	80)	08)	28)	22)	47)	24)	
0.8	2.92	2.95	3.89	2.98	4.30	9.14	10.3	13.3	14.2	21.5	26.3	31.6	21.8	26.8	34.0	26.8	32.4	42.8	
	(4.32)	(4.23)	(5.54)	(4.31)	(6.11)	(10.)	(11.)	(12.)	(12.)	(19.)	(20.)	(24.)	(18.)	(20.)	(27.)	(20.)	(25.)	(37.)	
)))))	56)	22)	11)	48)	87)	03)	82)	62)	67)	87)	07)	57)	39)	
0.7	2.00	2.01	2.52	2.02	2.70	5.17	5.80	7.44	8.11	10.8	13.8	15.7	11.0	13.7	16.3	13.9	16.0	19.8	
	(2.14)	(2.09)	(2.65)	(2.11)	(2.86)	(4.7)	(5.0)	(5.6)	(5.7)	(9.7)	(9.4)	(9.8)	(8.5)	(8.9)	(11.)	(8.6)	(10.)	(14.)	
)))))	8)	6)	2)	6)	3)	2)	7)	5)	1)	03)	2)	21)	84)	
0.5	1.25	1.24	1.44	1.26	1.51	2.52	2.80	3.55	3.85	3.89	5.52	6.55	4.23	5.58	6.44	5.82	6.53	7.03	
	(0.79)	(0.78)	(1.00)	(0.78)	(1.07)	(1.6)	(1.7)	(1.7)	(1.7)	(2.9)	(3.1)	(2.8)	(2.5)	(2.7)	(2.7)	(2.5)	(2.7)	(3.2)	
)))))	6)	4)	9)	8)	7)	3)	9)	4)	0)	5)	0)	4)	6)	
0.2	1.00	1.00	1.01	1.00	1.02	1.24	1.36	1.84	2.11	1.51	2.38	3.07	1.95	2.60	3.12	2.88	3.20	3.27	
5	(0.10)	(0.09)	(0.17)	(0.09)	(0.20)	(0.6)	(0.7)	(0.9)	(0.7)	(0.7)	(0.7)	(0.8)	(0.6)	(0.7)	(0.7)	(0.6)	(0.7)	(0.7)	
)))))	4)	4)	0)	5)	1)	9)	4)	7)	1)	3)	9)	0)	4)	
<i>EQL</i>		8.66	8.56	9.85	8.60	10.3	15.0	15.9	17.7	18.7	25.3	28.8	32.8	26.0	29.6	34.3	29.2	33.0	38.4
<i>RARL</i>		1.01	1.00	1.00	1.00	1.21	1.53	1.85	2.07	1.90	2.95	3.37	3.33	3.02	3.47	3.48	3.40	3.85	3.90
<i>PCI</i>		1.01	1.00	1.00	1.00	1.34	1.95	2.76	3.49	2.98	4.92	6.35	5.84	5.17	6.52	6.08	6.53	7.69	7.10
$\varphi =$		0.1	0.2	0.05	0.1	0.2	0.05	0.1	0.2	0.05	0.1	0.2	0.05	0.1	0.2	0.05	0.1	0.2	
$\delta =$		0.05	0.13	0.79	0.33	0.91	2.21	2.50	3.34	3.81	1.31	1.72	2.16	1.57	1.97	2.42	2.34	2.72	3.12
$L =$		0.139	32	4	3	5	1	4	7	9	6	6	8	6	4	8	5	8	
1	370.9	370.	370.	370.	370.	370.	369.	370.	370.	370.	370.	370.	370.	369.	370.	370.	370.	370.	
	7	13	61	06	49	05	96	61	81	91	55	31	88	61	97	33	52	99	
	(3675.)	(326)	(872.)	(194)	(752.)	(320)	(295)	(287)	(327)	(442)	(404)	(387)	(428)	(394)	(380)	(397)	(382)	(376)	
	48)	3.53)	67)	7.69)	39)	.54)	.75)	.22)	.03)	.16)	.97)	.38)	.66)	.60)	.36)	.99)	.01)	.81)	
1.0	31.46	30.0	107.	49.0	121.	220.	229.	250.	264.	198.	218.	238.	206.	225.	244.	220.	241.	261.	
25	8	35	1	97	24	94	11	91	84	96	15	29	78	50	92	75	45		
	(143.9)	(135.)	(240.)	(181.)	(241.)	(190)	(181.)	(186.)	(226)	(233)	(238)	(248)	(236)	(241)	(252)	(237)	(249)	(264)	
	4)	21)	15)	78)	89)	.03)	.03)	.14)	.48)	.31)	.21)	.70)	.26)	.30)	.70)	.49)	.21)	.52)	
1.0	15.00	15.1	52.2	23.1	61.0	145.	156.	179.	197.	123.	140.	162.	127.	147.	170.	143.	166.	192.	
5	5	9	2	2	29	60	59	25	10	40	35	82	32	36	52	19	12		
	(49.01)	(50.2)	(109.)	(68.2)	(115.)	(125)	(123)	(130)	(165)	(140)	(149)	(168)	(145)	(156)	(176)	(153)	(170)	(193)	
)	1)	40)	9)	96)	.85)	.21)	.32)	.60)	.85)	.81)	.05)	.40)	.51)	.24)	.56)	.81)	.41)	

Continued no next page

1.0	9.64	9.52	28.8	13.6	34.6	96.3	106.	128.	142.	77.5	91.2	108.	80.1	95.3	115.	93.1	112.	135.	
8			6	4	0	9	75	42	99	9	4	53	7	8	14	8	19	82	
	(24.94)	(24.5)	(56.1)	(33.4)	(62.0)	(84.)	(84.)	(90.)	(116)	(86.)	(96.)	(111)	(88.)	(100)	(117)	(97.)	(113)	(136)	
)	4)	8)	4)	0)	7)	67)	64)	.75)	99)	44)	.56)	82)	.56)	.8)	43)	.93)	.88)		
1.1	7.16	7.09	19.4	9.71	22.6	68.2	77.2	96.3	108.	54.2	63.5	76.7	55.0	66.0	82.0	64.3	78.9	99.8	
1			9	9	3	2	5	08	2	7	6	1	4	2	5	3	1		
	(15.44)	(15.2)	(34.9)	(20.2)	(38.7)	(60.)	(61.)	(66.)	(85.)	(59.)	(65.)	(77.)	(59.)	(68.)	(83.)	(66.)	(79.)	(99.)	
)	4)	4)	9)	3)	74)	90)	93)	78)	22)	26)	56)	85)	81)	49)	54)	51)	57)		
1.1	4.72	4.66	10.4	5.96	11.8	36.8	42.8	56.1	63.1	29.5	34.2	40.4	28.9	34.7	43.0	33.6	41.7	54.3	
8			3	8	8	4	5	1	0	2	8	8	7	2	4	6	1		
	(7.81)	(7.65)	(15.9)	(9.69)	(17.6)	(33.)	(35.)	(38.)	(47.)	(31.)	(33.)	(39.)	(30.)	(34.)	(42.)	(33.)	(40.)	(53.)	
)	7))	8)	68)	18)	14)	72)	55)	38)	23)	80)	38)	69)	50)	90)	62)			
1.2	3.65	3.61	7.07	4.46	8.02	23.1	27.2	37.2	41.2	19.1	21.9	25.4	18.4	21.9	26.6	21.0	25.9	33.6	
5				1	8	1	0	9	7	3	5	0	2	8	7	4			
	(5.03)	(4.92)	(9.55)	(6.15)	(10.5)	(21.)	(22.)	(25.)	(30.)	(20.)	(20.)	(23.)	(19.)	(21.)	(25.)	(20.)	(24.)	(32.)	
))))	3)	51)	95)	48)	21)	54)	64)	74)	17)	06)	55)	57)	34)	34)		
1.4	2.50	2.50	4.09	2.91	4.45	10.6	12.3	17.6	19.2	9.12	6	3	8.55	5	7	9.71	6	3	
3				2	6	4	6												
	(2.60)	(2.61)	(4.37)	(3.09)	(4.70)	(9.6)	(10.)	(12.)	(13.)	(9.9)	(10.)	(10.)	(8.8)	(9.4)	(10.)	(9.0)	(10.)	(12.)	
)))))	2)	59)	39)	50)	4)	08)	30)	4)	6)	50)	2)	29)	86)		
2	1.58	1.57	2.09	1.72	2.20	3.72	4.13	5.39	5.90	2.93	3.50	3.90	2.84	3.31	3.76	3.25	3.72	4.25	
	(1.19)	(1.18)	(1.68)	(1.35)	(1.76)	(2.8)	(3.1)	(3.8)	(4.0)	(3.0)	(3.3)	(3.3)	(2.6)	(2.9)	(3.0)	(2.6)	(2.9)	(3.3)	
)))))	6)	2)	1)	2)	5)	5)	5)	7)	3)	9)	4)	7)	3)		
4	1.11	1.10	1.21	1.13	1.23	1.52	1.60	1.82	1.85	1.22	1.30	1.38	1.24	1.31	1.39	1.35	1.43	1.51	
	(0.46)	(0.46)	(0.65)	(0.52)	(0.67)	(0.9)	(1.0)	(1.1)	(1.1)	(0.6)	(0.7)	(0.8)	(0.6)	(0.6)	(0.7)	(0.6)	(0.7)	(0.8)	
)))))	8)	4)	7)	4)	2)	3)	1)	0)	8)	6)	7)	5)	3)		
<i>EQL</i>	11.89		11.8	15.6	12.7	16.4	27.3	29.9	36.7	39.3	22.6	25.4	28.1	22.5	25.2	28.4	25.0	28.2	32.3
	0	3	6	7	6	0	2	8	1	5	5	2	8	3	5	7	6		
<i>RARL</i>	1.00	1.00	1.00	1.07	1.40	1.75	2.52	3.11	2.52	1.90	2.16	1.80	1.89	2.14	1.82	2.11	2.40	2.07	
<i>PCI</i>	1.00	1.00	1.00	1.10	1.51	1.86	3.19	4.16	2.89	2.32	2.70	1.94	2.27	2.65	1.93	2.58	3.01	2.24	

Table 6. ARL and SDRL values for the two-sided THWMA TBE chart and two-sided competing charts when $k = 3$ and $ARL_0 \cong 370$.

THWMA TBE				DHWMA TBE			HWMA TBE		TEWMA TBE			DEWMA TBE			EWMA TBE			
$\varphi =$	0.05	0.1	0.2	0.05	0.1	0.2	0.05	0.1	0.2	0.05	0.1	0.2	0.05	0.1	0.2	0.05	0.1	
δ	$L =$	1.249	1.56		1.342	1.63	2.41		2.26		3.35	1.74	2.03	2.35		1.94	2.23	2.53
	1.226	5	9		5	8		1				2	9	1		5	6	6
0.2	1.66	1.72	2.91	2.02	3.12	4.73	5.25	7.30	2.84	3.81	4.63	3.05	3.85	4.57	4.32	5.18		
5	(0.97)	(0.99)	(0.77)	(1.05)	(0.5)	(0.7)	(0.7)	(0.98)	(0.9)	(0.9)	(0.9)	(0.8)	(0.8)	(0.8)	(0.8)	(0.8)	(0.9)	
))))	9)	3)	9))	2)	7)	2)	0)	3)	3)	1)	2)		

Continued on next page

0.5	3.33	3.43	4.84	3.83	5.11	8.93	10.1 5	15.48	6.84	8.45	9.47	6.74	8.17	9.67	9.05	11.4 9	
	(1.90)	(1.91)	(2.03)	(1.94)	(2.0)	(3.0)	(3.2)	(4.45)	(3.7)	(3.6)	(3.3)	(3.1)	(3.2)	(3.6)	(3.2)	(4.2)	
))))	8)	4)	9))	5)	2)	7)	5)	0)	7)	7)	4)	
0.7	6.29	6.52	9.99	7.44	10.7	21.6	24.9	43.40	17.7	20.4	24.8	17.1	20.4	30.4	23.0	36.9	
	(5.25)	(5.39)	(7.18)	(5.88)	(7.5)	(11.)	(12.)	(19.5)	(11.)	(11.)	(15.)	(10.)	(11.)	(21.)	(12.)	(24.)	
))))	3)	26)	18)	2)	73)	27)	59)	55)	78)	69)	64)	74)	
0.8	10.18	10.66	18.2	20.0	43.7	50.9	114.6	34.2	40.0	59.9	34.0	43.8	84.7	49.3	109.		
	(11.4)	(11.8)	(17.2)	(13.3)	(18.)	(27.)	(30.)	(71.0)	(25.)	(28.)	(49.)	(24.)	(33.)	(75.)	(35.)	(95.)	
	2)	5)	8)	8)	38)	25)	00)	8)	06)	24)	88)	75)	07)	96)	05)	67)	
0.8	14.04	14.94	28.1	31.1	70.9	84.0	303.1	52.6	65.3	109.	54.3	75.2	162.	85.7	229.		
5		2	18.38	5	3	4	0	7	7	65	5	5	31	8	25		
	(19.0)	(20.0)	(30.9)	(23.3)	(32.)	(49.)	(55.)	(254.)	(42.)	(53.)	(100)	(44.)	(64.)	(155)	(70.)	(218)	
	2)	6)	0)	2)	76)	27)	29)	65)	29)	37)	.41)	33)	56)	.20)	57)	.38)	
0.9	21.79	23.44	50.7	56.8	139.	172.	2704.	95.0	125.	220.	102.	149.	323.	174.	492.		
	(37.8)	(40.2)	(66.1)	(48.6)	(70.)	(109)	(131)	(323)	(87.)	(117)	(214)	(95.)	(143)	(322)	(164)	(491)	
	1)	0)	6)	2)	02)	.66)	.00)	3.74)	62)	.41)	.73)	65)	.22)	.28)	.62)	.37)	
0.9	29.27	32.22	76.1	86.2	219.	280.	1855.	139.	184.	308.	151.	217.	426.	259.	631.		
25		5	43.60	9	10	24	15	05	03	14	40	80	77	84	64		
	(59.5)	(64.5)	(110.)	(80.1)	(116)	(182)	(227)	(173)	(138)	(180)	(306)	(150)	(215)	(430)	(254)	(637)	
	2)	4)	33)	9)	.93)	.92)	.49)	8.82)	.67)	.80)	.88)	.67)	.42)	.14)	.96)	.25)	
0.9	44.03	48.65	130.	69.11	146.	354.	449.	1012.	215.	272.	396.	232.	310.	486.	366.	648.	
5		17	69.11	98	47	51	55	30	92	09	74	87	02	52	52		
	(112.)	(121.)	(212.)	(151.)	(223)	(295)	(363)	(869.)	(229)	(280)	(401)	(244)	(317)	(491)	(371)	(658)	
	62)	16)	63)	94)	.35)	.19)	.75)	73)	.28)	.93)	.12)	.82)	.99)	.13)	.73)	.33)	
0.9	84.63	98.67	266.	147.8	289.	448.	502.	586.5	322.	362.	427.	338.	385.	461.	428.	521.	
75		79	5	70	34	56	0	21	65	71	20	72	74	08	26		
	(313.)	(346.)	(493.)	(433.)	(475)	(361)	(398)	(474.)	(362)	(381)	(439)	(370)	(404)	(470)	(447)	(529)	
	33)	47)	06)	46)	.99)	.71)	.34)	14)	.99)	.14)	.15)	.69)	.49)	.00)	.00)	.59)	
1	370.0	370.8	370.	371.3	370.	369.	368.	369.6	370.	370.	370.	369.	369.	370.	370.	369.	
	1	4	34	9	15	61	98	6	55	17	08	74	98	90	75	91	
	(3368)	(244)	(677.)	(137)	(593)	(300)	(288)	(286.)	(424)	(394)	(381)	(412)	(388)	(378)	(388)	(381)	
	.86)	4.97)	96)	5.52)	.91)	.78)	.67)	65)	.64)	.88)	.29)	.51)	.86)	.48)	.82)	.06)	
1.0	83.72	97.81	214.	141.3	224.	248.	245.	250.0	289.	289.	280.	289.	286.	272.	261.	251.	
25		03	5	72	48	54	3	07	77	87	63	46	23	42	96		
	(325.)	(348.)	(375.)	(402.)	(352)	(203)	(190)	(186.)	(330)	(308)	(289)	(324)	(301)	(278)	(276)	(259)	
	58)	54)	13)	22)	.70)	.03)	.15)	57)	.44)	.85)	.54)	.61)	.25)	.28)	.45)	.69)	
1.0	44.27	48.17	116.	69.47	126.	168.	169.	179.8	189.	200.	201.	192.	200.	194.	176.	176.	
5		41	52	07	58	6	74	87	64	06	81	34	46	59			

Continued no next page

	(119. 14)	(126. 24)	(188. 96)	(160. 67)	(188 .58)	(137 .41)	(130 .24)	(130. 70)	(210 .19)	(210 .05)	(206 .19)	(209 .24)	(210 .38)	(199 .27)	(184 .71)	(180 .30)		
1.0 8	27.38 30.09	66.3 9		73.0 39.61	112. 6	115. 33	128.1 73		117. 88	129. 17	136. 08	119. 11	129. 65	132. 69	113. 12	120. 07		
	(59.4 4)	(64.2 4)	(101. 18)	(78.1 0)	(103 .80)	(92. 99)	(88. 95)	(90.1 2)	(124 .77)	(132 .95)	(139 .16)	(126 .70)	(134 .10)	(135 .85)	(117 .07)	(122 .50)		
1.1 1	19.73 21.39	43.6 1		27.54 9	48.0 8	80.1 1	83.7 96.33		79.6 6	87.6 6	95.0 6	79.5 5	88.1 9	93.9 5	78.4 4	84.0 9		
	(37.1 7)	(39.3 6)	(63.1 9)	(48.6 1)	(65. 55)	(66. 79)	(64. 94)	(66.9 8)	(80. 98)	(87. 57)	(95. 70)	(82. 14)	(90. 06)	(95. 13)	(79. 66)	(84. 64)		
1.1 8	11.87 12.63	21.7 2		15.07 5	23.8 4	42.7 2	46.2 56.19		41.4 9	44.6 1	48.3 4	39.7 9	44.1 3	48.7 0	39.7 2	43.8 6		
	(17.7 7)	(18.8 4)	(28.1 9)	(21.6 8)	(30. 20)	(36. 94)	(36. 88)	(38.1 1)	(39. 64)	(41. 65)	(46. 63)	(38. 86)	(42. 54)	(48. 06)	(38. 61)	(42. 78)		
1.2 5	8.54 8.90	13.7 6		10.34 8	14.9 5	26.8 3	29.4 37.16		26.4 8	27.8 2	29.3 4	24.6 7	26.9 9	29.4 6	24.3 1	27.2 0		
	(11.1 6)	(11.6 0)	(16.2 6)	(13.1 0)	(17. 56)	(23. 64)	(23. 96)	(25.3 9)	(24. 98)	(24. 95)	(27. 18)	(23. 52)	(25. 00)	(28. 24)	(22. 88)	(25. 74)		
1.4 3	5.04 (5.24)	5.16 (5.36)	6.95 (7.00)	5.69 (5.88)	7.29 (7.3)	11.9 (10.)	13.3 9	17.47 0	12.3 0	12.9 6	13.1 7	11.0 3	11.9 5	12.7 0	10.8 4	11.9 2		
									(11. 12)	(12.2 7)	(11. 07)	(11. 42)	(11. 22)	(10. 50)	(10. 61)	(11. 25)	(9.8. 2)	(10. 57)
2	2.48 (1.98)	2.51 (2.00)	2.92 (2.32)	2.63 (2.10)	3.00 (2.3)	4.01 (3.0)	4.30 (3.2)	5.39 (3.84)	3.70 (3.7)	4.07 (3.7)	4.22 (3.5)	3.43 (3.1)	3.74 (3.2)	3.94 (3.2)	3.50 (2.8)	3.79 (3.0)		
									(7) 3)	(4) 1)	(8) 6)	(6) 5)	(4) 2)	(2) 3)	(3) 1)			
4	1.31 (0.78)	1.31 (0.78)	1.38 (0.87)	1.33 (0.81)	1.40 (0.8)	1.59 (1.0)	1.64 (1.0)	1.81 (1.16)	1.30 (0.7)	1.37 (0.8)	1.43 (0.8)	1.31 (0.6)	1.36 (0.7)	1.42 (0.7)	1.38 (0.7)	1.44 (0.7)		
									(8) 1)	(4) 1)	(8) 6)	(1) 3)	(7) 2)	(9) 5)	(9) 1)			
<i>EQL</i>	16.35	16.81	22.9	16.60	24.0	34.3	37.3	78.31	30.3	33.1	37.3	29.9	33.2	39.9	33.1	43.8		
<i>RARI</i>	1.00	1.00	1.00	1.02	1.43	1.50	2.28	4.66	1.86	1.97	1.63	1.83	1.98	1.74	2.03	2.61		
<i>PCI</i>	1.00	1.00	1.00	1.01	1.38	1.52	2.40	4.69	1.88	2.04	1.64	1.82	2.00	1.71	2.08	2.75		

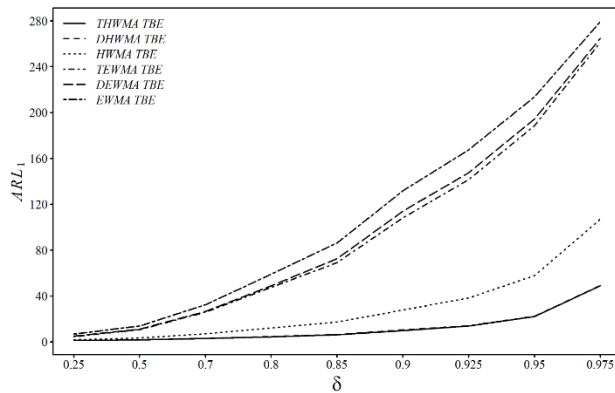


Figure 1. ARL_1 plot for the lower-sided THWMA TBE versus lower-sided competing charts when $k = 1$, $\varphi = 0.05$ and $ARL_0 = 370$.

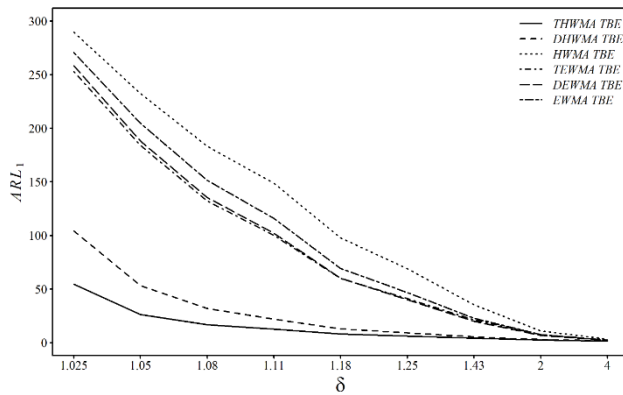


Figure 2. ARL_1 plot for the upper-sided THWMA TBE versus upper-sided competing charts when $k = 1$, $\varphi = 0.05$ and $ARL_0 = 370$.

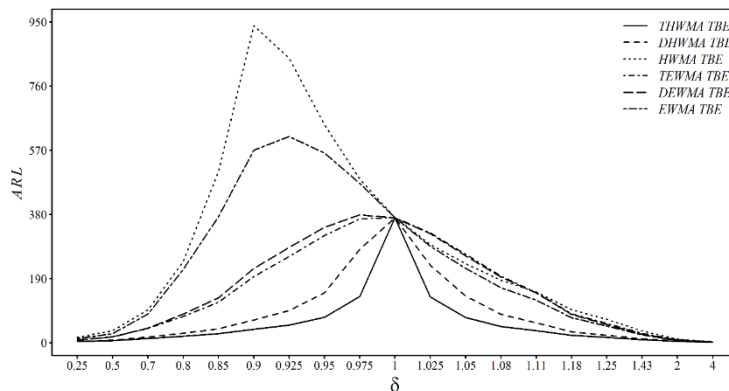


Figure 3. ARL plot for the two-sided THWMA TBE versus two-sided competing charts when $k = 1$, $\varphi = 0.05$ and $ARL_0 = 370$.

5. Applications of THWMA TBE chart

This section provides two real-life examples to demonstrate how THWMA TBE charts can be used practically. Subsection 5.1 offers Example 5.1, which analyzes real-life data of a vertical boring machine's failure time. Additionally, the analysis of the real-life data representing the hospital stay time of the traumatic brain injury patients is given in Subsection 5.2.

5.1. Example 5.1

Boring machines are extensively utilized in boring, drilling, milling, thread cutting, face-turning processes, etc. These machines may be horizontal or vertical, depending on the axis. The boring machines use a spinning tool known as a machine spindle, which generates the basic motion. By enlarging the existing holes in the workpiece, these machines generate a smooth and precise hole diameter. To accomplish this, boring machines employed a cutter, boring rod, drill or milling head to bore, thread, ream and mill surfaces, among other operations. A single steel cutting tip, a diamond, cemented carbide or a tiny grinding wheel can be used as the boring instrument. Special boring machines with many spindles are often utilized in large production plants [28].

In this example, the dataset is analyzed that reports the vertical boring machine failure times. This dataset was also utilized by Hossain et al. [29] and Hossain et al. [30] to construct various chart schemes. The TBE charts are not only implemented to monitor the processes of components or systems [8] in addition to being utilized to monitor the boring machine failure process. All possible actions must be taken to maintain the capability of the boring process to reduce the expense and hardship of boring machine failure.

Table 7 shows the data set, which consists of 32 vertical boring machine failure time (in hours) observations. Before implementing the THWMA TBE charts, the Kolmogorov-Smirnov (KS) test is used to test the goodness-of-fit for the gamma distribution. The KS test provides a p -value of 0.3053, which confirms that the boring machine failure time follows the gamma distribution at the parametric values $k = 3$ and $\theta = 959.3$. To implement the THWMA TBE charts, the methodology of Alevizakos and Koukouvinos [11] is followed. The IC value θ_0 of the process is considered to be 1200 for the downward shift, and for the upward shift, it is assumed to be 800. As a result, the shifts δ for downward and upward cases are approximately equal to 0.8 and 1.2, respectively. Because the earlier developments assume $\theta_0 = 1$, so each observation in Table 7 is divided by θ_0 to rescale the failure time. Setting $ARL_0 = 370$, the lower-sided THWMA TBE, DHWMA TBE, HWMA TBE, TEWMA TBE, DEWMA TBE and EWMA TBE charts are constructed using the design parameters for each chart, respectively chosen as; $(\varphi, L) = (0.2, 0.453)$, $(\varphi, L) = (0.2, 1.027)$, $(\varphi, L) = (0.2, 1.498)$, $(\varphi, L) = (0.2, 1.885)$, $(\varphi, L) = (0.2, 2.027)$ and $(\varphi, L) = (0.2, 2.117)$ (see Table 5). Similarly, the upper-sided THWMA TBE, DHWMA TBE, HWMA TBE, TEWMA TBE, DEWMA TBE and EWMA TBE charts are formulated, based on the design parameters, respectively, given as; $(\varphi, L) = (0.2, 0.794)$, $(\varphi, L) = (0.2, 2.211)$, $(\varphi, L) = (0.2, 3.819)$, $(\varphi, L) = (0.2, 2.168)$, $(\varphi, L) = (0.2, 2.424)$ and $(\varphi, L) = (0.2, 3.128)$ (see Table 5). Likewise, the two-sided THWMA TBE, DHWMA TBE, HWMA TBE, TEWMA TBE, DEWMA TBE and EWMA TBE charts are developed, which used the design parameters provided as; $(\varphi, L) = (0.05, 1.226)$, $(\varphi, L) = (0.05, 1.342)$, $(\varphi, L) = (0.05, 2.261)$, $(\varphi, L) = (0.05, 1.742)$, $(\varphi, L) = (0.05, 1.945)$ and $(\varphi, L) = (0.05, 2.524)$, respectively (see Table 6). The lower, upper and two-sided THWMA TBE, DHWMA TBE, HWMA TBE, TEWMA TBE,

DEWMA TBE and EWMA TBE charts are displayed in Figures 4–6, respectively.

Figure 4 reveals that the lower-sided THWMA TBE chart detects the first OOC point at failure number 7, while the lower-sided DHWMA TBE, HWMA TBE and TEWMA TBE charts diagnose the first OOC point at failure numbers 11, 23 and 20, respectively; however, the lower-sided DHWMA TBE and EWMA TBE charts fail to identify any OOC point. Similarly, Figure 5 indicates that the upper-sided THWMA TBE chart detects the first OOC point at failure number 3, while the upper-sided DHWMA TBE and TEWMA TBE charts identify the first OOC point at failure numbers 27 and 3, respectively, and the upper-sided HWMA TBE and EWMA TBE charts remain insensitive and do not detect any OOC signal. Likewise, Figure 6 suggests that with decreasing shift, the two-sided THWMA TBE chart provides the first OOC signal at failure number 16, while the two-sided DHWMA TBE chart triggers the first OOC point at failure number 19, but the HWMA TBE, TEWMA TBE, DEWMA TBE and EWMA TBE charts detect no OOC point. Equally, Figure 6 also shows that, with increasing shift, both the two-sided THWMA TBE and DHWMA TBE charts produce the first OOC point at failure number 4, whereas both the two-sided HWMA TBE and DEWMA TBE charts diagnose the OOC point at failure number 27 and the TEWMA TBE and EWMA TBE charts identify no OOC signal. The above discussion suggests that the THWMA TBE charts are more efficient in detecting changes in the process than the DHWMA TBE, HWMA TBE, TEWMA TBE, DEWMA TBE and EWMA TBE charts.

Table 7. Vertical boring machine failure time (in hours).

Sample no.	Failure time						
1	2802	9	2937	17	2136	25	4359
2	4020	10	1781	18	2816	26	2655
3	3886	11	2296	19	3158	27	3695
4	4155	12	3811	20	2380	28	376
5	2172	13	3705	21	2848	29	4339
6	2076	14	2672	22	3632	30	1976
7	1700	15	1596	23	1701	31	3575
8	3802	16	4351	24	4291	32	808

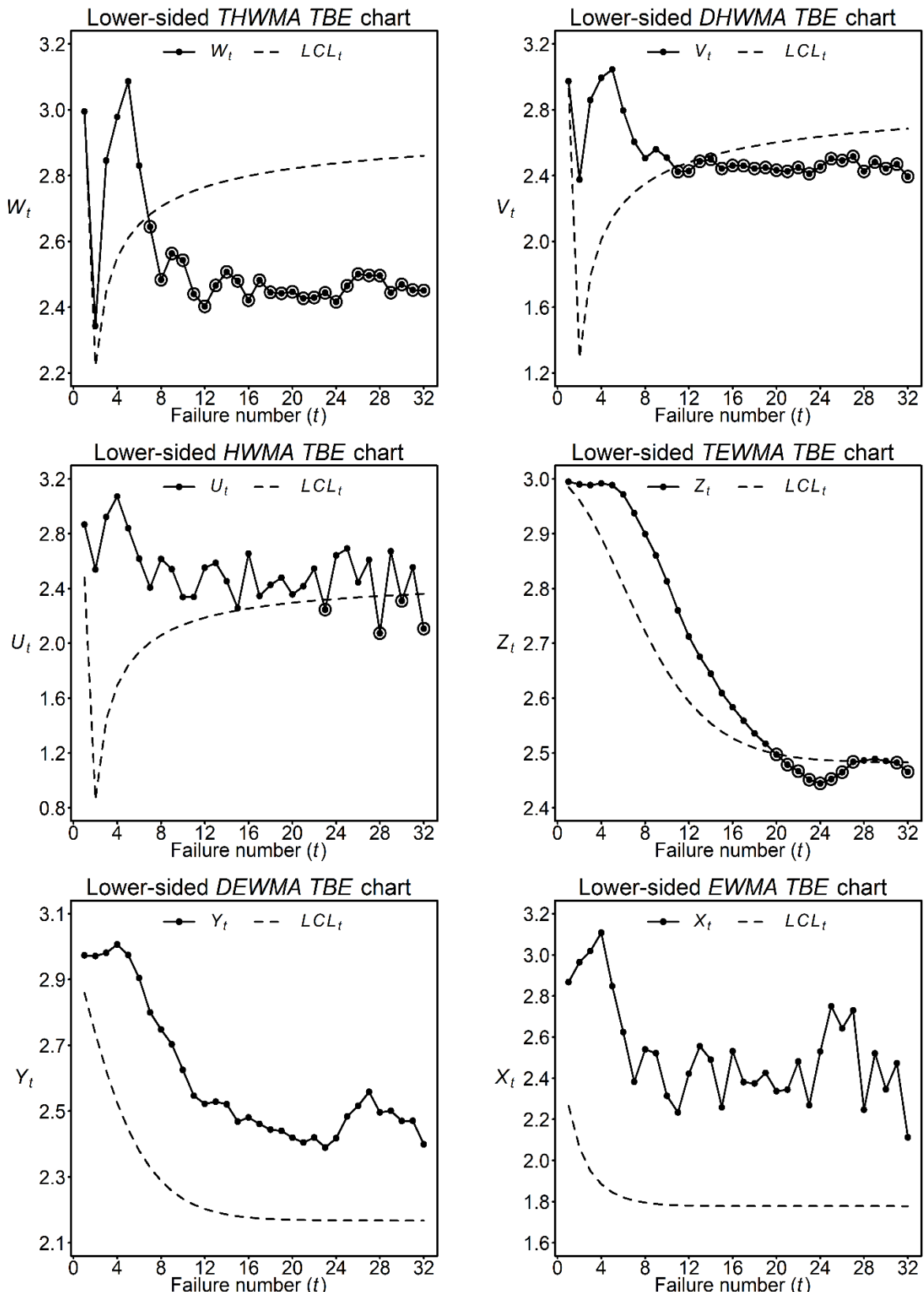


Figure 4. Lower-sided THWMA TBE chart and lower-sided competing charts for Example 5.1 data with $\varphi = 0.2$ and $\delta = 0.8$.

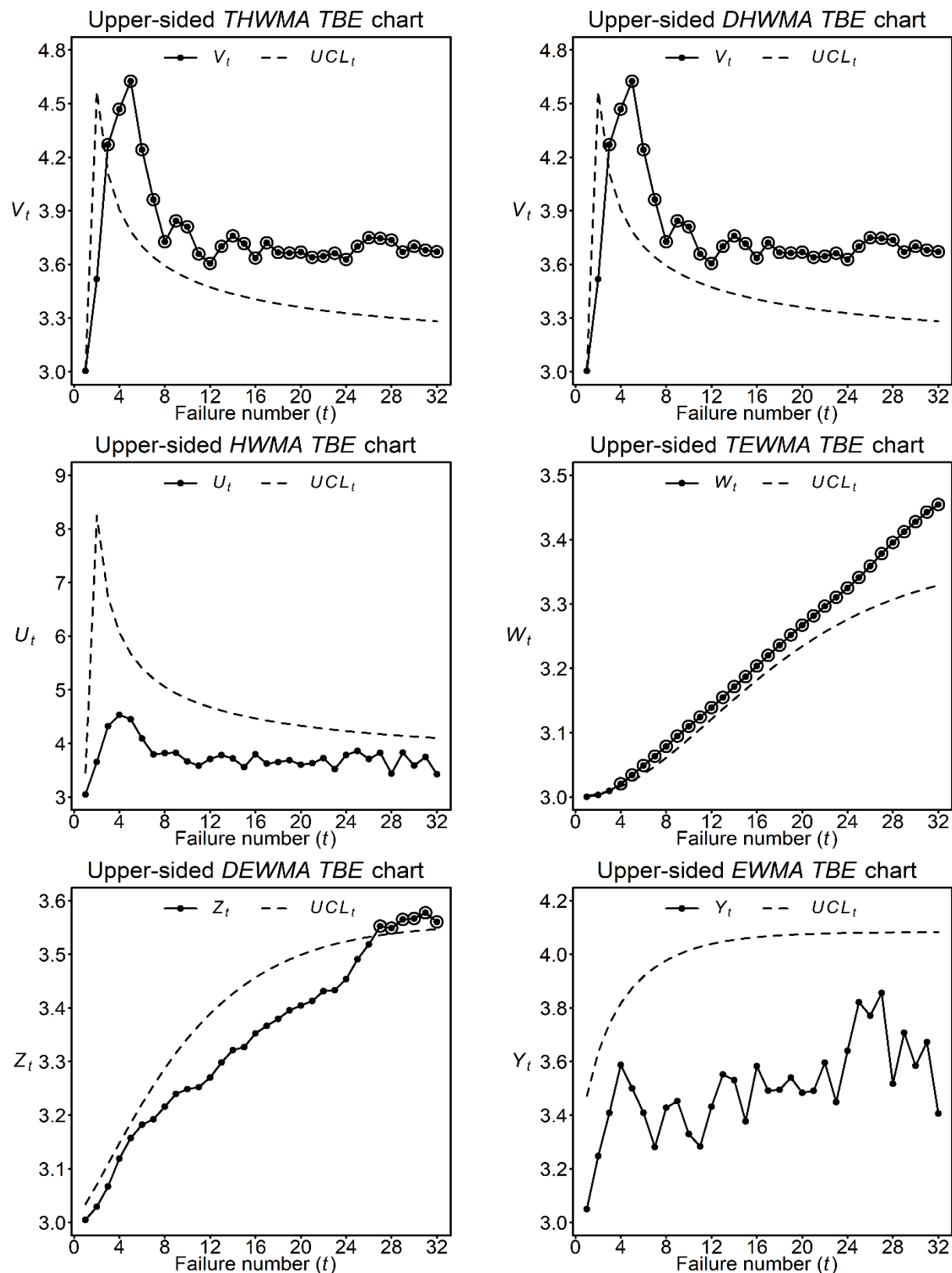


Figure 5. Upper-sided THWMA TBE chart and upper-sided competing charts for Example 5.1 data with $\varphi = 0.2$ and $\delta = 1.2$.

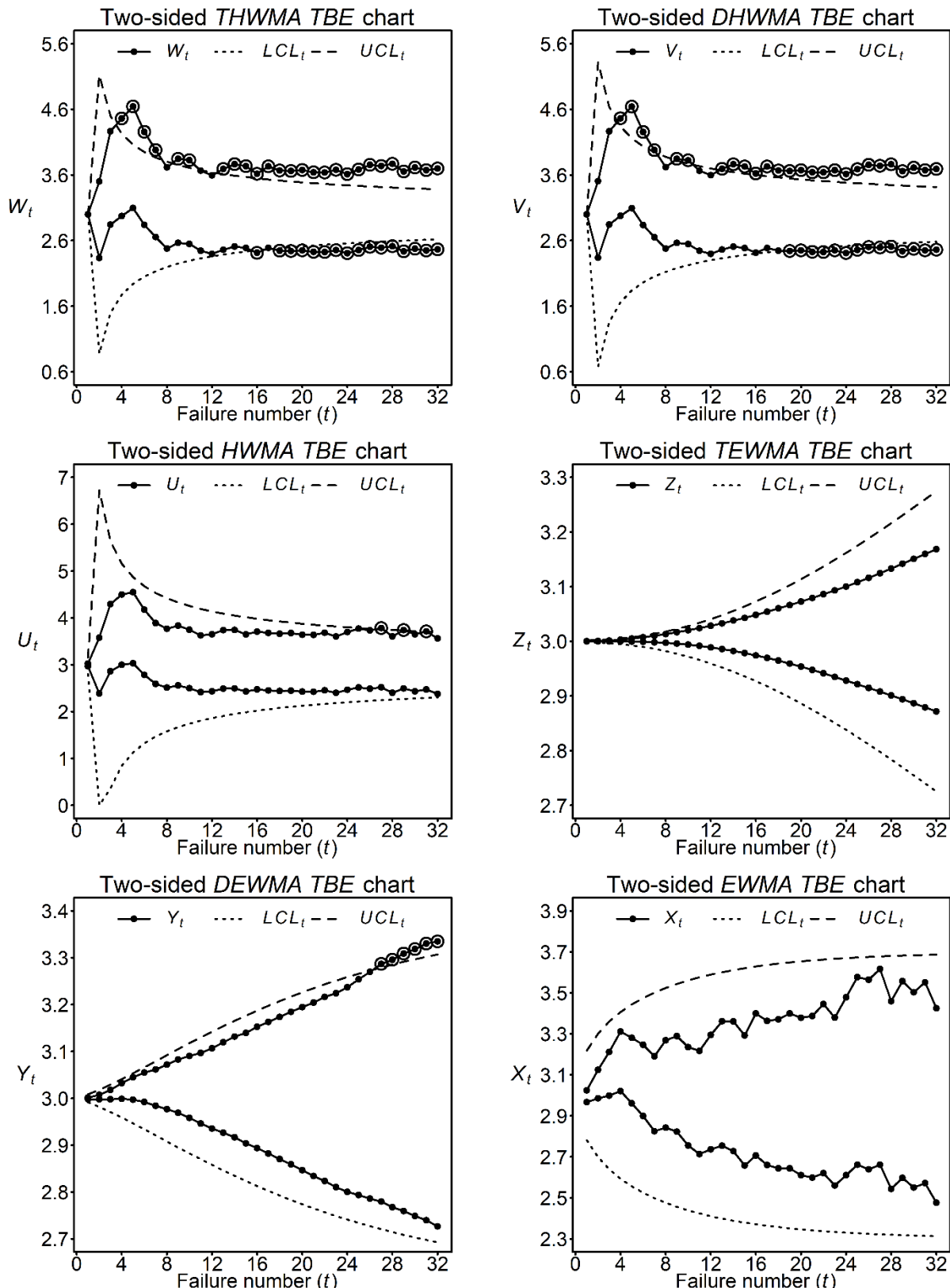


Figure 6. Two-sided THWMA TBE chart and two-sided competing charts for Example 5.1 data with $\varphi = 0.05$ and $\delta = 1.2$.

5.2. Example 5.2

Trauma is a multifaceted psychiatric state that is the third leading source of mortality globally, after only cardiovascular disease and cancer. As a result of traumatic injury, over sixty million individuals are believed to be affected by trauma every year, with approximately 16,000 people dying each day. In trauma epidemiology statistics, traumatic brain injury (TBI) is one of the main roots of death and disability [31]. The vast majority of TBI patients are young and financially active adults who have a higher risk of being involved in road accidents [32]. As a result, TBI is viewed as a public health issue that results in large healthcare costs as well as many economic and social impacts. Therefore, a monitoring scheme is needed to assist in developing public health policies, reduce the TBI burden and enhance survival. In the current example, the one- and two-sided THWMA TBE with the competing charts, i.e., DHWMA TBE, HWMA TBE, TEWMA TBE, DEWMA TBE and EWMA TBE charts are applied to the data set of male patients suffering from TBI related to car accidents, hospitalized in the Emergency Department of Ribeirão Preto Medical School, University of São Paulo, Brazil.

The data set considered by Ramos et al. [33] representing the hospital stay time for male patients suffering from TBI related to car accidents is offered in Table 8. The KS goodness-of-fit test is applied, which provides a p -value of 0.918, confirming that the hospital stay times of the TBI patients follow the gamma distribution having parameters $k = 1$ and $\theta = 32.5$. In accordance with Alevizakos et al. [2], the IC process value θ_0 is supposed to be 50 for the decrease in interarrival time; however, for the increase in interarrival time, it is considered to be 15. As a result, the data set may be regarded as the OOC process observations having a decreasing shift of size 0.65 and an increasing shift of size 2.17. All the previous developments are executed at $\theta_0 = 1$, thus each observation of the data set is divided by the IC value θ_0 , i.e., $\theta_0 = 50$ for the downward shift and $\theta_0 = 15$.

Table 8. Hospital stay time for male patients suffering from TBI related to car accidents.

Patient number	Hospital stay	Patient number	Hospital stay	Patient number	Hospital stay
1	25	8	19	15	44
2	6	9	6	16	65
3	20	10	35	17	39
4	12	11	23	18	4
5	23	12	35	19	50
6	6	13	21		
7	67	14	15		

The THWMA TBE, DHWMA TBE, HWMA TBE, TEWMA TBE, DEWMA TBE and EWMA TBE charts are constructed with a common value of ARL_0 , i.e., $ARL_0 \cong 370$. The design parameters; $(\varphi, L) = (0.2, 0.365)$, $(\varphi, L) = (0.2, 0.727)$, $(\varphi, L) = (0.2, 0.9537)$, $(\varphi, L) = (0.2, 1.7765)$, $(\varphi, L) = (0.2, 1.8724)$ and $(\varphi, L) = (0.05, 1.813)$ are, respectively, chosen to formulate the lower-sided THWMA TBE, DHWMA TBE, HWMA TBE, TEWMA TBE, DEWMA TBE and EWMA TBE charts. The lower-sided charts are shown in Figure 7, which suggests that the lower-sided THWMA TBE chart diagnoses the first OOC signal after patient number 1, whereas the lower-sided D DHWMA TBE, HWMA TBE, TEWMA TBE and DEWMA TBE charts, respectively, diagnose the first OOC

point after patient numbers 2, 2, 10 and 13, but the EWMA TBE chart detects no OOC point. In addition, Figure 7 also indicates that the THWMA TBE chart overall detects 18 OOC signals, while the DHWMA TBE, HWMA TBE, TEWMA TBE and DEWMA TBE charts trigger 17, 17, 9 and 2 OOC signals, respectively.

Similarly, the upper-sided THWMA TBE, DHWMA TBE, HWMA TBE, TEWMA TBE, DEWMA TBE and EWMA TBE charts are developed using the design parameters, respectively, given as; $(\varphi, L) = (0.2, 0.878)$, $(\varphi, L) = (0.2, 2.608)$, $(\varphi, L) = (0.2, 4.601)$, $(\varphi, L) = (0.2, 2.258)$, $(\varphi, L) = (0.2, 2.548)$ and $(\varphi, L) = (0.2, 3.498)$. The upper-sided charts are depicted in Figure 8, which indicates that the upper-sided THWMA TBE chart identifies the first OOC point at patient number 7, while the upper-sided DHWMA TBE, TEWMA TBE, DEWMA TBE and EWMA TBE charts, respectively, trigger the first OOC point after patient numbers 15, 15, 16 and 15, but the HWMA TBE chart fails to detect any OOC signal. Furthermore, Figure 8 also demonstrates that the THWMA TBE chart diagnoses 14 OOC points in total; however, the DHWMA TBE, TEWMA TBE, DEWMA TBE and EWMA TBE charts detect 4, 4, 3 and 3 OOC points, respectively.

Likewise, the two-sided THWMA TBE, DHWMA TBE, HWMA TBE, TEWMA TBE, DEWMA TBE and EWMA TBE charts are constructed, which are based on the design parameters; $(\varphi, L) = (0.05, 1.196)$, $(\varphi, L) = (0.05, 1.342)$, $(\varphi, L) = (0.05, 2.998)$, $(\varphi, L) = (0.05, 1.724)$, $(\varphi, L) = (0.05, 1.9264)$ and $(\varphi, L) = (0.05, 2.536)$. The two-sided charts are portrayed in Figure 9, which demonstrates that both two-sided THWMA TBE and DHWMA TBE charts trigger the first OOC point after patient numbers 4 and 7 with downward and upward shift, respectively; however, the two-sided DEWMA TBE chart identifies the first OOC signal after patient number 13 with downward and after patient number 15 with upward shifts, respectively. On the other hand, the two-sided HWMA TBE and EWMA TBE charts diagnose the first OOC point after patient numbers 16 and 15, respectively, with an upward shift only, while the two-sided TEWMA TBE chart is unable to detect the OOC signal. Moreover, in overall detection, Figure 9 also shows that the two-sided THWMA TBE and DHWMA TBE charts detect 15 OOC signals with decreasing shift, whereas the two-sided DEWMA TBE chart trigger 6 OOC points. On the contrary, as the increasing shift is concerned, the two-sided THWMA TBE and DHWMA TBE charts detect 11 OOC points, whereas the two-sided HWMA TBE, DEWMA TBE and EWMA TBE charts identify 3, 4 and 3 OOC points, respectively. The above discussion suggests that, in terms of the ability to diagnose the changes in the process, the THWMA TBE appears to be more sensitive than other charts, i.e., the DHWMA TBE, HWMA TBE, TEWMA TBE, DDEWMA TBE, and EWMA TBE charts.

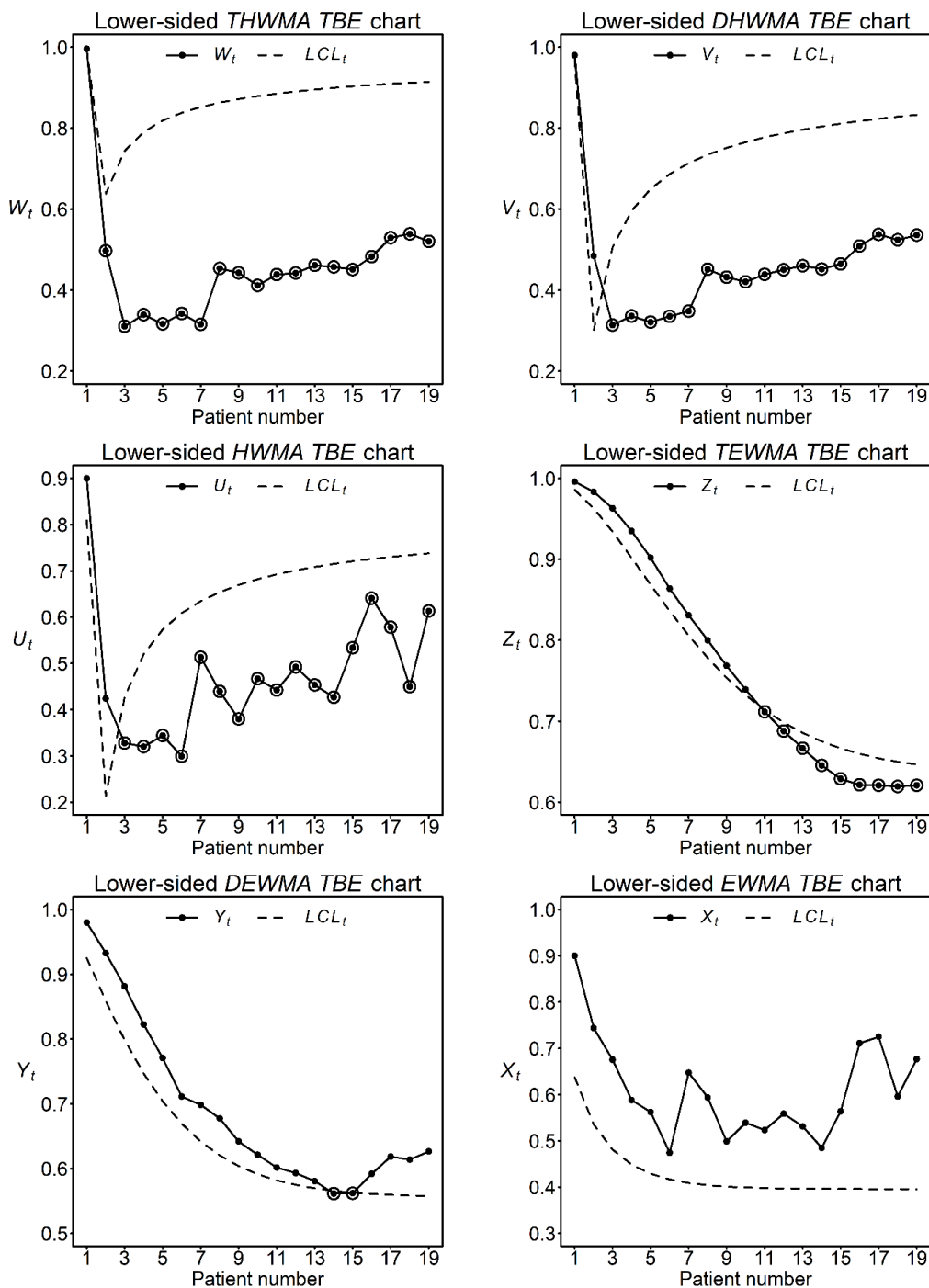


Figure 7. Lower-sided THWMA TBE chart versus lower-sided competing charts for Example 5.2 data with $\varphi = 0.2$ and $\delta = 0.65$.

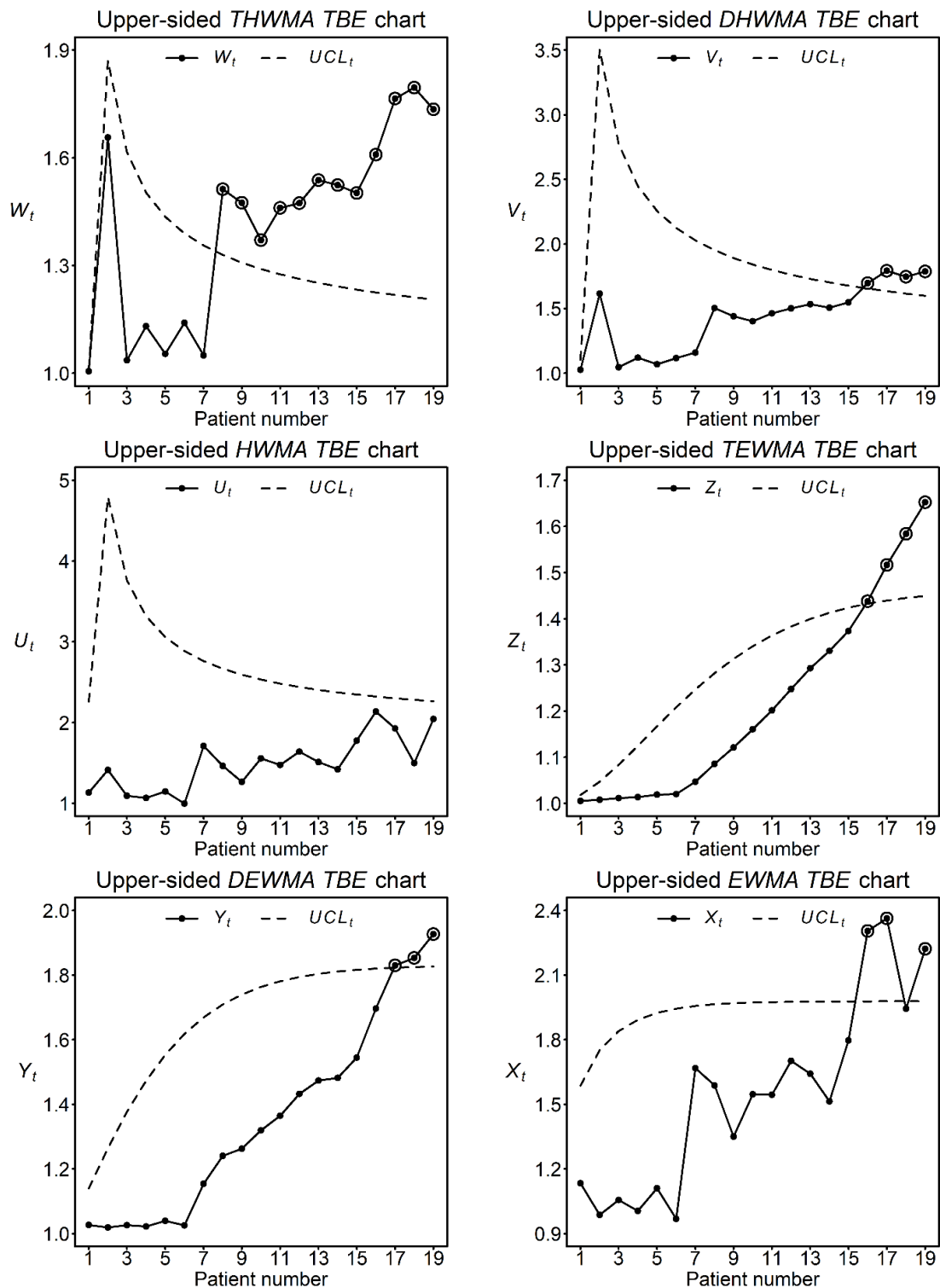


Figure 8. Upper-sided THWMA TBE chart versus upper-sided competing charts for Example 5.2 data with $\varphi = 0.2$ and $\delta = 2.17$.

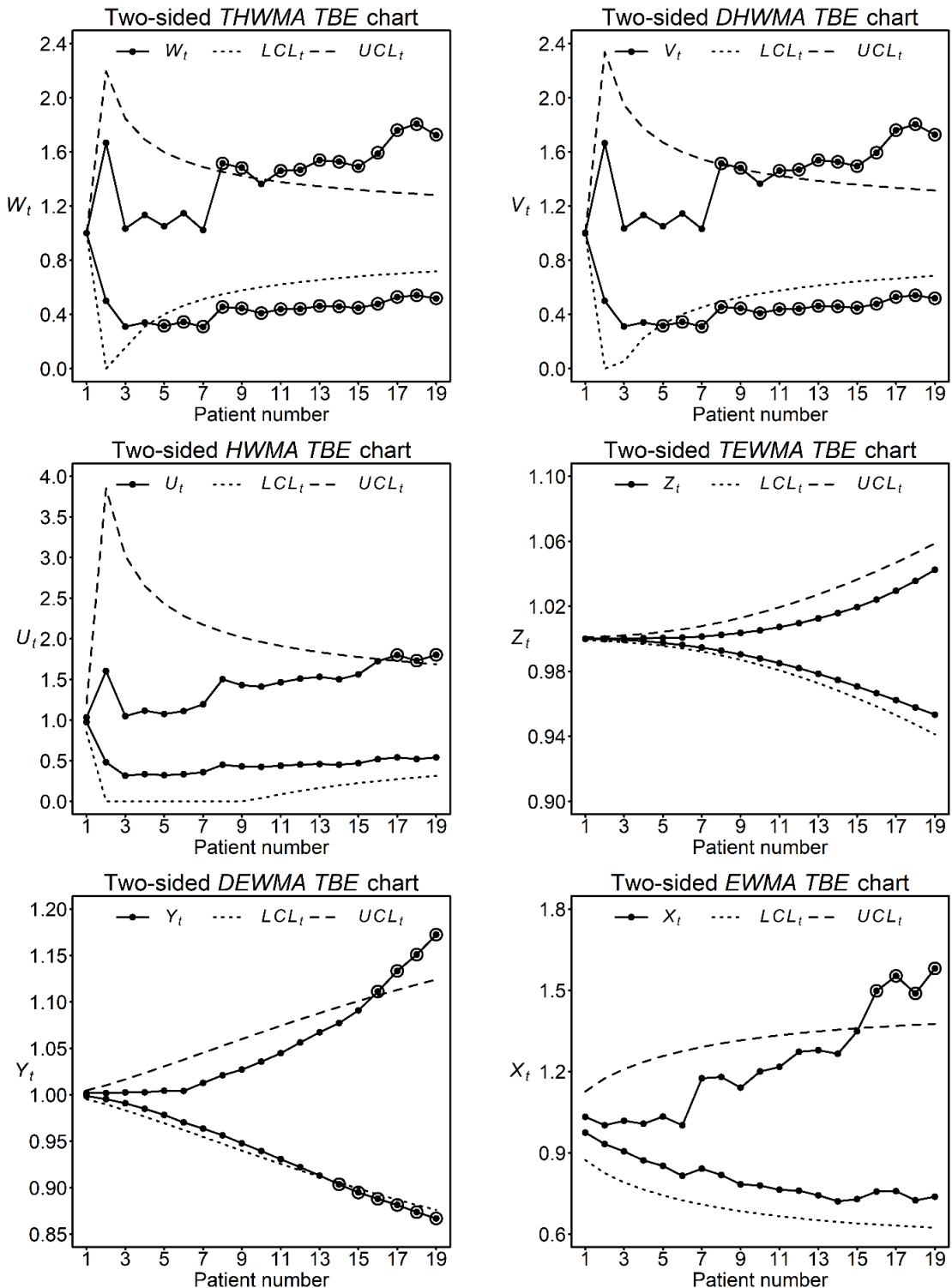


Figure 9. Two-sided THWMA TBE chart versus two-sided competing charts for Example 5.2 data with $\varphi = 0.05$ and $\delta = 0.65, 2.17$.

6. Conclusions, summary and recommendations

This paper proposes triple homogeneously weighted moving average charts to monitor TBE observations following by the gamma distribution. The proposed charts are referred to as THWMA

TBE charts. THWMA TBE charts are one- and two-sided charts. The one-sided THWMA TBE charts comprise the lower- and upper-sided THWMA TBE charts, which monitor the process's downward and upward shifts, respectively. Similarly, the two-sided THWMA TBE chart detects both the downward and upward changes in the process simultaneously. The Monte Carlo simulations methodology is used to compute the numerical findings for the performance measures, such as average run length (ARL), standard deviation run length (SDRL), extra quadratic loss (EQL), relative average run length (RARL) and performance comparison index (PCI). These numerical findings are obtained for the THWMA TBE charts, as well as for competing charts including the DHWMA TBE, HWMA TBE, TEWMA TBE, DEWMA TBE and EWMA TBE charts. A comparison study, based on aforementioned performance measures, is carried out and the THWMA TBE charts are compared to the competing charts. The comparison suggests that the THWMA TBE charts outperform the competing DHWMA TBE, HWMA TBE, TEWMA TBE, DEWMA TBE and EWMA TBE charts. In addition, two real-life data sets, i.e., one representing vertical boring machine failure time, and the other representing the hospital stay time for traumatic brain injury patients, are analyzed to implement the one- and two-sided THWMA TBE charts practically. Finally, it is pointed out that some of the issues may require further research. For instance, the performance of the THWMA TBE charts can be investigated in the case when the scale parameter of the gamma distribution is assumed to be unknown and thus estimated by the reference sample or historical data. Furthermore, the THWMA TBE methodology can be used in cases when TBE observations follow distributions such as Weibull or lognormal.

Use of AI tools declaration

The authors declare they have not used Artificial Intelligence (AI) tools in the creation of this article.

Acknowledgments

This research was supported by the Princess Nourah bint Abdulrahman University Researchers Supporting Project number (PNURSP2023R259), Princess Nourah bint Abdulrahman University, Riyadh, Saudi Arabia.

Conflict of interest

The authors reported that they do not have any conflicts of interest.

Availability of Data and Materials

Open source data sets are used and references are provided.

References

1. W. A. Shewhart, *Economic control of quality of manufactured product*, New York: D. Van Nostrand Company, 1931.

2. V. Alevizakos, C. Koukouvinos, A. Lappa, Monitoring of time between events with a double generally weighted moving average control chart, *Qual. Reliab. Eng. Int.*, **35** (2019), 685–710. <https://doi.org/10.1002/qre.2430>
3. M. Aslam, M. Khan, S. M. Anwar, B. Zaman, A homogeneously weighted moving average control chart for monitoring time between events, *Qual. Reliab. Eng. Int.*, **38** (2022), 1013–1044. <https://doi.org/10.1002/qre.3032>
4. J. M. Lucas. Counted data CUSUM's, *Technometrics*, **27** (1985), 129–144.
5. S. Vardeman, D. Ray, Average run lengths for CUSUM schemes when observations are exponentially distributed, *Technometrics*, **27** (1985), 145–150.
6. F. F. Gan, Designs of one- and two-sided exponential EWMA charts, *J. Qual. Technol.*, **30** (1998), 55–69. <https://doi.org/10.1080/00224065.1998.11979819>
7. L. Y. Chan, M. Xie, T. N. Goh, Cumulative quantity control charts for monitoring production processes, *Int. J. Prod. Res.*, **38** (2000), 397–408. <https://doi.org/10.1080/002075400189482>
8. M. Xie, T. N. Goh, P. Ranjan, Some effective control chart procedures for reliability monitoring, *Reliab. Eng. Syst. Safe.*, **77** (2002), 143–150. [https://doi.org/10.1016/S0951-8320\(02\)00041-8](https://doi.org/10.1016/S0951-8320(02)00041-8)
9. C. Pehlivan, M. C. Testik, Impact of model misspecification on the exponential EWMA charts: a robustness study when the time-between-events are not exponential, *Qual. Reliab. Eng. Int.*, **26** (2010), 177–190. <https://doi.org/10.1002/qre.1033>
10. N. Chakraborty, S. W. Human, N. Balakrishnan, A generally weighted moving average chart for time between events, *Commun. Stat.-Simul. Comput.*, **46** (2017), 7790–7817. <https://doi.org/10.1080/03610918.2016.1252397>
11. V. Alevizakos, C. Koukouvinos, A double exponentially weighted moving average chart for time between events., *Commun. Stat.-Simul. Comput.*, **49** (2000), 2765–2784. <https://doi.org/10.1080/03610918.2018.1532516>
12. V. Alevizakos, K. Chatterjee, C. Koukouvinos, A triple exponentially weighted moving average control chart for monitoring time between events, *Qual. Reliab. Eng. Int.*, **37** (2021), 1059–1079. <https://doi.org/10.1002/qre.2781>
13. S. W. Roberts, Control chart tests based on geometric moving averages, *Technometrics*, **42** (2000), 97–101.
14. J. S. Hunter, The exponentially weighted moving average, *J. Qual. Technol.*, **18** (1986), 203–210. <https://doi.org/10.1080/00224065.1986.11979014>
15. N. Abbas, Homogeneously weighted moving average control chart with an application in substrate manufacturing process, *Comput. Ind. Eng.*, **120** (2018), 460–470. <https://doi.org/10.1016/j.cie.2018.05.009>
16. M. Abid, A. Shabbir, H. Z. Nazir, R. A. K. Sherwani, M. Riaz, A double homogeneously weighted moving average control chart for monitoring of the process mean, *Qual. Reliab. Eng. Int.*, **36** (2020), 1513–1527.
17. M. Riaz, Z. Abbas, H. Z. Nazir, M. Abid, On the development of triple homogeneously weighted moving average control chart, *Symmetry*, **13** (2021), 360. <https://doi.org/10.3390/sym13020360>
18. Z. Rasheed, H. Y. Zhang, S. M. Anwar, B. Zaman, Homogeneously mixed memory charts with application in the substrate production process, *Math. Prob. Eng.*, **2021** (2021), 2582210. <https://doi.org/10.1155/2021/2582210>

19. Z. Rasheed, H. Y. Zhang, M. Arslan, B. Zaman, S. M. Anwar, M. Abid, et al., An efficient robust nonparametric triple EWMA Wilcoxon signed-rank control chart for process location, *Math. Probl. Eng.*, **2021** (2021), 2570198. <https://doi.org/10.1155/2021/2570198>
20. Z. Rasheed, M. Khan, N. L. Abiodun, S. M. Anwar, G. Khalaf, S. A. Abbasi, Improved nonparametric control chart based on ranked set sampling with application of chemical data modelling, *Math. Probl. Eng.*, **2022** (2022), 7350204. <https://doi.org/10.1155/2022/7350204>
21. V. Alevizakos, C. Koukouvinos, A progressive mean control chart for monitoring time between events, *Qual. Reliab. Eng. Int.*, **36** (2020), 161–186. <https://doi.org/10.1002/qre.2565>
22. V. Alevizakos, C. Koukouvinos, Monitoring reliability for a gamma distribution with a double progressive mean control chart, *Qual. Reliab. Eng. Int.*, **37** (2021), 199–218. <https://doi.org/10.1002/qre.2730>
23. D. C. Montgomery, *Introduction to Statistical Quality Control*, Hoboken: John Wiley & Sons, 2013.
24. M. Awais, A. Haq, A new cumulative sum control chart for monitoring the process mean using varied L ranked set sampling, *J. Ind. Prod. Eng.*, **35** (2018), 74–90. <https://doi.org/10.1080/21681015.2017.1417787>
25. Z. Wu, J. X. Jiao, M. Yang, Y. Liu, Z. J. Wang, An enhanced adaptive Cusum control chart, *IIE Trans.*, **41** (2009), 642–653. <https://doi.org/10.1080/07408170802712582>
26. M. Khan, M. Aslam, S. M. Anwar, B. Zaman, A robust hybrid exponentially weighted moving average chart for monitoring time between events, *Qual. Reliab. Eng. Int.*, **38** (2022), 895–923. <https://doi.org/10.1002/qre.3021>
27. Y. J. Ou, Z. Wu, F. Tsung, A comparison study of effectiveness and robustness of control charts for monitoring process mean, *Int. J. Prod. Econ.*, **135** (2012), 479–490.
28. P. N. Rao, *Manufacturing Technology: Metal Cutting and Machine Tools*, McGraw-Hill Education (India) Pvt Limited, 2000.
29. M. P. Hossain, M. H. Omar, M. Riaz, New V control chart for the Maxwell distribution, *J. Stat. Comput. Sim.*, **87** (2016), 594–606. <https://doi.org/10.1080/00949655.2016.1222391>
30. M. P. Hossain, R. A. Sanusi, M. H. Omar, M. Riaz, On designing Maxwell CUSUM control chart: an efficient way to monitor failure rates in boring processes, *Int. J. Adv. Manuf. Technol.*, **100** (2019), 1923–1930.
31. R. H. Bonow, J. Barber, N. R. Temkin, W. Videtta, C. Rondina, G. Petroni, et al., The outcome of severe traumatic brain injury in Latin America, *World Neurosurg.*, **111** (2018), e82–e90. <https://doi.org/10.1016/j.wneu.2017.11.171>
32. P. W. Owens, N. P. Lynch, D. P. O’Leary, A. J. Lowery, M. J. Kerin, Six-year review of traumatic brain injury in a regional trauma unit: demographics, contributing factors and service provision in Ireland, *Brain Injury*, **32** (2018), 900–906. <https://doi.org/10.1080/02699052.2018.1466366>
33. P. L. Ramos, D. C. Nascimento, P. H. Ferreira, K. T. Weber, T. E. G. Santos, F. Louzada, Modeling traumatic brain injury lifetime data: Improved estimators for the generalized Gamma distribution under small samples, *Plos One*, **14** (2019), e0221332.

Supplementary

Appendix A: Mean, variance, and covariance of T_t

Suppose $T_i^* \stackrel{iid}{\sim} \text{Exponential}(\theta)$ for $i = 1, 2, \dots, k$ and if $T = \sum_{i=1}^k T_i^*$ then $T \sim \text{Gamma}(k, \theta)$.

Let $T_t \stackrel{iid}{\sim} \text{Gamma}(k, \theta)$ at time $t = 1, 2, \dots$ then for the IC process, i.e., $\theta = \theta_0$,

$$E(T_t) = k\theta_0, \text{Var}(T_t) = k\theta_0^2 \text{ and } \text{Cov}(T_t, T_s) = 0 \text{ for all } t, s = 1, 2, \dots \text{ and } t \neq s. \quad (\text{A1}).$$

For the IC process, the expected value of \bar{T}_t is given as follows:

$$\begin{aligned} E(\bar{T}_t) &= \frac{1}{t-1} E\left(\sum_{j=1}^t T_j\right) \\ &= \frac{1}{t} E(T_1 + T_2 + \dots + T_t) \\ &= \frac{1}{t} [E(T_1) + E(T_2) + \dots + E(T_t)] = k\theta_0 \end{aligned} \quad (\text{A2})$$

Similarly, the variance of \bar{T}_t is given as follows:

$$\begin{aligned} \text{Var}(\bar{T}_t) &= \frac{1}{t^2} \text{Var}\left(\sum_{j=1}^t T_j\right) \\ &= \frac{1}{t^2} [\sum_{j=1}^t \text{Var}(T_j) + 2 \sum_{j < l} \text{Cov}(T_j, T_l)] \\ &= \frac{1}{t^2} [k\theta_0^2 + k\theta_0^2 + \dots + k\theta_0^2] = \frac{k\theta_0^2}{t}. \end{aligned} \quad (\text{A3})$$

Likewise, the covariance of T_t and \bar{T}_{t-1} , i.e., $\text{Cov}(T_t, \bar{T}_{t-1})$ is given as follows:

$$\begin{aligned} \text{Cov}(T_t, \bar{T}_{t-1}) &= \text{Cov}\left(T_t, \frac{T_1 + T_2 + \dots + T_{t-1}}{t-1}\right) \\ &= \frac{1}{t-1} [\text{Cov}(T_t, T_1) + \text{Cov}(T_t, T_2) + \dots + \text{Cov}(T_t, T_{t-1})] \\ &= \frac{1}{t-1} [0 + 0 + \dots + 0] = 0. \end{aligned} \quad (\text{A4})$$

Appendix B: Mean and variance of HWMA TBE chart

The charting statistic of the HWMA TBE chart is presented as follows:

$$U_t = \varphi T_t + (1 - \varphi) \bar{T}_{t-1} \quad (\text{B1})$$

For a stable process, the mean of U_t is given as follows:

$$\begin{aligned} E(U_t) &= E[\varphi T_t + (1 - \varphi) \bar{T}_{t-1}] \\ &= \varphi E(T_t) + (1 - \varphi) E(\bar{T}_{t-1}) \\ &= \varphi k\theta_0 + (1 - \varphi) k\theta_0 = k\theta_0 \end{aligned} \quad (\text{cf. Eq. A1 and A2})$$

Similarly, the variance of U_t is provided as follows:

$$\begin{aligned} \text{Var}(U_t) &= \text{Var}[\varphi T_t + (1 - \varphi) \bar{T}_{t-1}] \\ &= \varphi^2 \text{Var}(T_t) + (1 - \varphi)^2 \text{Var}(\bar{T}_{t-1}) + 2\varphi(1 - \varphi) \text{Cov}(T_t, \bar{T}_{t-1}) \\ &= \varphi^2 k\theta_0^2 + (1 - \varphi)^2 \frac{k\theta_0^2}{t-1} + 2\varphi(1 - \varphi)(0) \quad (\text{cf. Eq. A1, A3, and A4}) \end{aligned}$$

$$= \left\{ \varphi^2 + \frac{(1-\varphi)^2}{t-1} \right\} k\theta_0^2$$

or

$$Var(U_t) = \varphi^2 k\theta_0^2, \text{ if } t = 1, \text{ and } Var(U_t) = \left\{ \varphi^2 + \frac{(1-\varphi)^2}{t-1} \right\} k\theta_0^2, \text{ if } t > 1.$$

Appendix C: Mean and variance of DHWMA TBE chart

The DHWMA TBE statistic, V_t can be defined as follows:

$$\begin{aligned} V_t &= \varphi U_t + (1 - \varphi) \bar{T}_{t-1} \quad (\text{C1}) \\ &= \varphi [\varphi T_t + (1 - \varphi) \bar{T}_{t-1}] + (1 - \varphi) \bar{T}_{t-1} \quad (\text{cf. Eq B1}) \\ &= \varphi^2 T_t + (1 - \varphi^2) \bar{T}_{t-1} \quad (\text{C2}) \end{aligned}$$

For the IC process, the mean of V_t is defined as follows:

$$\begin{aligned} E(V_t) &= E[\varphi^2 T_t + (1 - \varphi^2) \bar{T}_{t-1}] \\ &= \varphi^2 E(T_t) + (1 - \varphi^2) E(\bar{T}_{t-1}) \\ &= \varphi^2 k\theta_0 + (1 - \varphi^2) k\theta_0 = k\theta_0 \quad (\text{cf. Eq A1 and A2}) \end{aligned}$$

In the same way, the variance of V_t is defined as follows:

$$\begin{aligned} Var(V_t) &= Var[\varphi^2 T_t + (1 - \varphi^2) \bar{T}_{t-1}] \\ &= \varphi^4 Var(T_t) + (1 - \varphi^2)^2 Var(\bar{T}_{t-1}) + 2\varphi^2(1 - \varphi^2) Cov(T_t, \bar{T}_{t-1}) \\ &= \varphi^4 k\theta_0^2 + \frac{(1-\varphi^2)^2 k\theta_0^2}{t-1} + 2\varphi^2(1 - \varphi^2)(0) \quad (\text{cf. Eq A1, A3, and A4}) \\ &= \left\{ \varphi^4 + \frac{(1-\varphi^2)^2}{t-1} \right\} k\theta_0^2 \end{aligned}$$

or

$$Var(V_t) = \varphi^4 k\theta_0^2, \text{ if } t = 1, \text{ and } Var(V_t) = \left\{ \varphi^4 + \frac{(1-\varphi^2)^2}{t-1} \right\} k\theta_0^2, \text{ if } t > 1.$$

Appendix D: Mean and variance of THWMA TBE chart

The plotting statistic of the THWMA TBE chart is defined as follows:

$$W_t = \varphi V_t + (1 - \varphi) \bar{T}_{t-1} \quad (\text{D1})$$

$$= \varphi [\varphi^2 T_t + (1 - \varphi^2) \bar{T}_{t-1}] + (1 - \varphi) \bar{T}_{t-1} \quad (\text{cf. Eq C2})$$

$$= \varphi^3 T_t + (1 - \varphi^3) \bar{T}_{t-1} \quad (\text{D2})$$

The IC mean of W_t is given as follows:

$$\begin{aligned} E(W_t) &= E[\varphi^3 T_t + (1 - \varphi^3) \bar{T}_{t-1}] \\ &= \varphi^3 E(T_t) + (1 - \varphi^3) E(\bar{T}_{t-1}) \\ &= \varphi^3 k\theta_0 + (1 - \varphi^3) k\theta_0 = k\theta_0 \quad (\text{cf. Eq A1 and A2}) \end{aligned}$$

Similarly, the IC variance of W_t is given as follows:

$$\begin{aligned}
Var(W_t) &= Var[\varphi^3 T_t + (1 - \varphi^3) \bar{T}_{t-1}] \\
&= \varphi^6 Var(T_t) + (1 - \varphi^3)^2 Var(\bar{T}_{t-1}) + 2\varphi^3(1 - \varphi^3) Cov(T_t, \bar{T}_{t-1}) \\
&= \varphi^6 k \theta_0^2 + \frac{(1-\varphi^3)^2 k \theta_0^2}{t-1} + 2\varphi^3(1 - \varphi^3)(0) \quad (\text{cf. Eq A1, A3, and A4}) \\
&= \left\{ \varphi^6 + \frac{(1-\varphi^3)^2}{t-1} \right\} k \theta_0^2
\end{aligned}$$

or

$$Var(W_t) = \varphi^6 k \theta_0^2, \text{ if } t = 1, \text{ and } Var(W_t) = \left\{ \varphi^6 + \frac{(1-\varphi^3)^2}{t-1} \right\} k \theta_0^2, \text{ if } t > 1.$$



AIMS Press

© 2023 the Author(s), licensee AIMS Press. This is an open access article distributed under the terms of the Creative Commons Attribution License (<http://creativecommons.org/licenses/by/4.0>)